

## Response to anonymous Referee #2

### Summary:

This paper presents and analyzes a large data set that is a 10-year record of ozone and CO measurements at 7 sites in the northeast U.S. The authors have done a wide variety of analyses, described in long discussions, but in the end, they can draw no firm conclusions. The work as it stands has major shortcomings. I suggest that this paper be rejected. The following comments describe my concerns.

We would like to thank the reviewer for their comments on the article. We now defined “baseline” in the abstract and introduction explicitly and more clearly, reorganized figures and tables, and emphasized the quality control of measurement data that were used in the study. Detailed point-to-point response to the reviewer’s comments was provided as follows.

### Major issues:

1) The title of the paper emphasizes my first concern. The term "baseline" concentration has a specific meaning, which I believe was originally defined in the 2009 HTAP Report entitled "Hemispheric Transport Of Air Pollution 2010:

"A baseline concentration is an observation made at a site when it is not influenced by recent, locally emitted or produced pollution. These baseline sites are typically situated in locations with minimal and infrequent impact from local sources of anthropogenic pollution. Observations may be made continuously and subsequently sorted, or air samples taken only when meteorological conditions are such that the recorded concentrations are free from the local contamination. Time series of baseline concentrations provide the range and frequency of pollutant concentrations transported to the site from upwind locations. However the requirement that only recently emitted or produced local pollution be excluded means that baseline concentrations may contain traces of local pollutants that were emitted many days earlier and became well-mixed with other air masses. There is no strict definition of “recently” emitted or produced local sources of anthropogenic pollution."

The current paper selects data to analyze that is labeled "baseline" but in fact no means was identified to determine the influence of "locally emitted or produced pollution". I do not believe that it is possible to determine baseline concentrations of CO or ozone at any site in the northeastern US, since the region is surrounded by pollutant sources, and most of the North American continent lies upwind of that region. Furthermore, characterization of baseline concentrations requires defining the distribution of concentrations that are measured under baseline conditions. They may be low concentrations, but they may also be high concentrations. For example, baseline concentrations of CO may be elevated if anthropogenic emissions or wildfire emissions are transported to the site from a distant continent, and baseline

concentrations of ozone may be greatly elevated if a stratospheric intrusion is transported to the site.

It is the reviewer's opinion that it is impossible to determine baseline concentrations of CO or O<sub>3</sub> at any site in the northeastern US. We disagree with that. In a multi-year time series of CO, the baseline is simply the line that consists of the lowest values of certain time intervals, be daily or monthly. An example is shown in Figure S2. We gave this baseline a range by using monthly 10<sup>th</sup> percentile values. There is no policy connotation intended in the term "baseline" used in this study.

There is clearly a lack of a universal definition of baseline CO or O<sub>3</sub> in the scientific community. The 2009 HTAP report was a great effort to present the consensus of such definitions from the community's decades of research. During the past three decades, a great number of studies have investigated the trends and variability in background or baseline O<sub>3</sub> (e.g., Altshuller, 1987; Altshuller and Lefohn, 1996; Cooper et al., 2010; Cui et al., 2011; Derwent et al., 2007; Jaffe et al., 2003; Lin et al., 2000; Logan et al., 2012; Parrish et al., 2009; Wilson et al., 2012). Background and baseline are used, often interchangeably, to quantify how much O<sub>3</sub> produced from recent or local anthropogenic emissions could be allowed to attain the O<sub>3</sub> standards (HTAP, 2010; Huang et al., 2015). A few recent studies discussed the difference between background O<sub>3</sub> and baseline O<sub>3</sub> (Chan and Vet, 2010; HTAP, 2010; Huang et al., 2015; Parrish et al., 2012). The term "background" was used in modeling studies that estimated the atmospheric mixing ratio of a compound determined by natural sources only (HTAP, 2010; Chan et al., 2010; Parrish et al., 2012; Huang et al., 2015). Parrish et al. (2010) pointed out that the US Environmental Protection Agency (EPA) used a similar term, Policy Relevant Background (PRB), which was defined as O<sub>3</sub> that would exist in the absence of North American anthropogenic emissions. Fiore et al., (2002) defined background O<sub>3</sub> as O<sub>3</sub> produced outside the North American boundary layer (surface to 700 hPa) and naturally formed O<sub>3</sub> within the U.S., using a three-dimensional global tropospheric chemistry model (GEOS-Chem). Huang et al. (2015) estimated western U.S. background O<sub>3</sub> by zeroing out the U.S. anthropogenic emissions in the regional Sulfur Transport and dEposition Model (STEM). However, it is impossible to quantify this type of background O<sub>3</sub> using observational data, as the effect of North American emissions is inherently included in ambient measurements (Chan et al., 2010; Parrish et al., 2010).

The term "baseline" referred to concentration levels of compounds at times when fresh/local emission influences were negligible and can be obtained from measurement records by removing data of local influences (HTAP, 2010; Chan et al., 2010; Parrish et al., 2012; Huang et al., 2015). Various methods have been utilized to diagnose baseline conditions, including measurements at remote sites, analysis of the probability distribution of pollutants, and correlations with reactive nitrogen oxides (e.g. Altshuller and Lefohn, 1996; Lin et al., 2000; Jaffe et al., 2003; Derwent et al., 2007; Parrish et al., 2009; Cui et al., 2011; Wilson et al., 2012). Here are a few examples using measurement data from remote sites or rural sites, which are in geographic approximation from urban/industrial source regions that are similar to our sites. Lin et al. (2000) analyzed the

probability distribution of O<sub>3</sub> concentrations at U.S. rural sites over 1980 – 1998 and defined baseline O<sub>3</sub> concentrations as the median values for the lowest 25<sup>th</sup> percentiles of CO and NO<sub>y</sub> concentrations. Jaffe et al. (2003) extracted baseline data from the total dataset by selecting time periods of high winds from the direction of the Pacific coast and isentropic back-trajectories that has not in contact with the continent for more than 24 hours. Derwent et al. (2007) used halocarbons and CO to identify polluted air masses at Mace Head and used the NAME Lagrangian dispersion model to exclude times when air masses were from east of Mace Head or southern latitudes, or when the air was not well mixed around the station. Parrish et al. (2009) selected baseline conditions when samples were collected during a high, onshore local wind window. Cui et al. (2011) selected baseline conditions at Jungfraujoch by running 20-day back trajectories and air masses without contact with the European boundary layer were considered baseline periods. Wilson et al. (2012) used the 5<sup>th</sup> percentile value of O<sub>3</sub> mixing ratios as a measure of the baseline or background conditions.

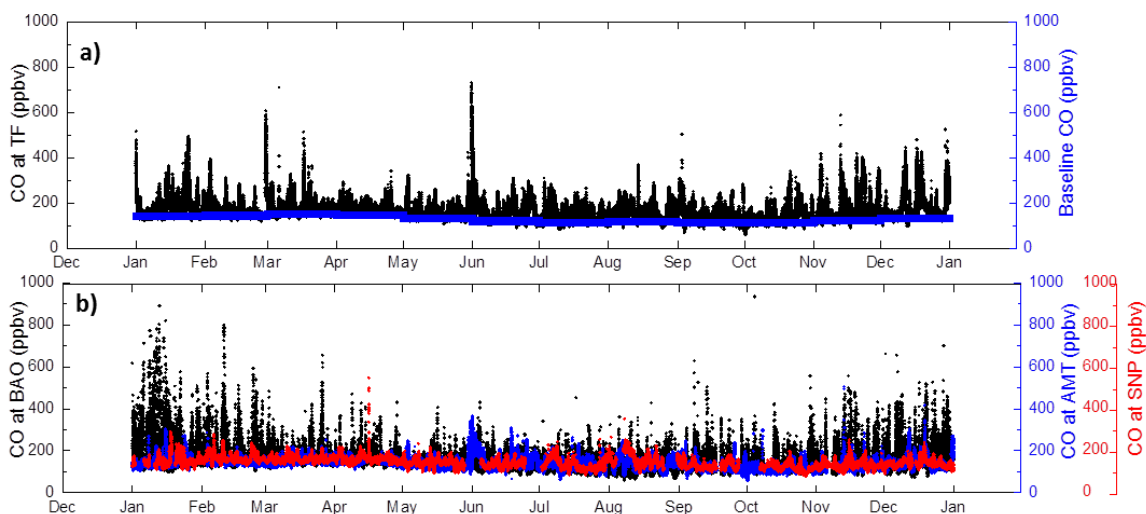


Figure S2 (a). Time series of 1-min CO (ppbv) and monthly baseline CO (ppbv) at TF in 2010. (b) Time series of 5-min CO (ppbv) at BAO, AMT, and SNP in 2010.

In our study, all the seven sites are located in rural areas of the Northeast U.S. They are ~100 km far away from the Northeast urban corridor and at least ~200 km away from the Ohio River Valley, the major industrial region in the Northeast US. We estimated the baseline CO and baseline O<sub>3</sub> using criteria similar to that from Lin et al. (2000), Mao et al. (2008), Mao and Talbot, (2012). Baseline CO was determined using the monthly 10<sup>th</sup> percentile level of CO at low elevation rural sites and 50<sup>th</sup> percentile at the two mountain sites. Monthly median O<sub>3</sub> levels of the baseline air were defined as baseline O<sub>3</sub> levels. We only used the data during daytime when the convective boundary layer is fully developed and measurements at a surface site was more regionally representative. Specifically, Figure S2 shows time series of 1-min CO and monthly baseline CO at TF in 2010. Monthly baseline CO quantified by our method was able to track the variation of the low level CO mixing ratios at this site (Figure S2a). Using the dataset from the NOAA Earth System Research Laboratory Global Monitoring Division, we found annual

averaged CO was 138 ppbv at Argyle, Maine (AMT), 140 ppbv at Boulder, Colorado (BAO), and 148 ppbv at Shenandoah National Park, Virginia (SNP) (Figure S2b). Seasonal cycles at these three sites were similar to those found at TF, which had the maximum value of 150 ppbv in March and the minimum value of 111 ppbv in September. As demonstrated in Section 3.3.1, baseline CO mixing ratios over our study region were significantly impacted by wildfires in Russia and Canada. Specifically, owing to expansive wildfires in Siberia, baseline CO in summer 2003 was 130 ppbv at AI, 171 ppbv at MWO, 148 ppbv at TF, 187 ppbv at PSP, and 183 ppbv at WFM, where were much higher than in normal years.

Baseline O<sub>3</sub> mixing ratios from our study ranged from 28 – 56 ppbv over 2001 – 2010, which were consistent with values of US continental background O<sub>3</sub> (35±10 ppbv in summer and 45±10 ppbv in early spring) estimated using various techniques in other studies (Altshuller and Lefohn, 1996; Lin et al., 2000; Jaffe et al., 2003; Parrish et al., 2009; Chan et al., 2010). Although baseline O<sub>3</sub> was obtained by correlation with low mixing ratios of CO, baseline O<sub>3</sub> quantified by our method could be still influenced by stratospheric intrusion. Stratospheric air masses contain high mixing ratios of O<sub>3</sub> and very low mixing ratios of CO (Schroeder et al., 2014). Thus stratospheric intrusion can lead to dilution of surface CO and decrease CO levels, which were most likely captured by the monthly 10<sup>th</sup> percentile criteria.

To reflect the investigative work in this study, the title was changed to “Regional and Hemispheric Influences on Variability and Trends of Baseline Carbon Monoxide and Ozone over the Northeast US”.

At the beginning of the abstract, we added the definition of baseline CO and O<sub>3</sub>: “Baseline carbon monoxide (CO) and ozone (O<sub>3</sub>) were defined as mixing ratios of CO and O<sub>3</sub> under minimal influence of recent and local emissions. In this study, baseline carbon monoxide (CO) and ozone (O<sub>3</sub>) were examined at seven rural sites in the Northeast US during varying periods over 2001–2010. Specifically, baseline air was determined using the monthly 10<sup>th</sup> percentile level of CO at Appledore Island (AI), Castle Spring (CS), Pack Monadnock (PM), Thompson Farm (TF), Pinnacle State Park (PSP), and 50<sup>th</sup> percentile level at Mt. Washington (MWO) and Whiteface Mountain (WFM). Monthly median O<sub>3</sub> levels of the baseline air were defined as baseline O<sub>3</sub> levels.” (L28 – L35)

To clarify the definition of baseline, we added the following sentences in the Introduction:

“Background or baseline has been used, often interchangeably, to quantify how much O<sub>3</sub> produced from recent or local anthropogenic emissions could be allowed to attain the O<sub>3</sub> standards (HTAP, 2010; Huang et al., 2015). A few recent studies discussed the difference between background O<sub>3</sub> and baseline O<sub>3</sub> (HTAP, 2010; Huang et al., 2015; Parrish et al., 2012; Chan et al., 2010). The term “background” was used in modeling studies that estimated the atmospheric mixing ratio of a compound determined by natural sources only, while the term

“baseline” was obtained from measurement records by removing data of local influences (HTAP, 2010, Chan et al., 2010; Parrish et al., 2012).” (L108 – L115)

“Various methods have been utilized to diagnose baseline conditions, including using measurements at remote sites, analysis of the probability distribution of pollutants, correlations with reactive nitrogen oxides, and isentropic back-trajectories (e.g., Altshuller and Lefohn, 1996; Lin et al., 2000; Jaffe et al., 2003; Derwent et al., 2007; Parrish et al., 2009; Cui et al., 2011; Wilson et al., 2012).” (L117 – L121)

2) What the authors attempt to do in this paper is to determine monthly average concentrations of an approximate regional background of CO and O<sub>3</sub>. It may be that a useful paper could be written discussing such background concentrations, and how they vary with the many variables that the authors consider. However, even such an analysis is compromised because the authors are not successful in describing a regional background that is actually regional. This is clear from Figure 2 where time series of the results are plotted. The background concentrations of CO and ozone determined for each of the seven sites are not the same. There are certainly similarities, but there are also large, unexplained differences. In my view, the authors must reconsider their analysis to arrive at two time series: one a monthly average regional background CO concentration, and the other a monthly average regional background ozone concentration. It is not clear to me that this can be achieved, but in Figure 2 there appears to be enough similarity between sites that it may be possible to derive time series that represent a regional background for the northeastern US.

The baseline CO and O<sub>3</sub> were defined as CO and O<sub>3</sub> measured at surface sites without the influence of strong local effects. Therefore, baseline CO and baseline O<sub>3</sub> could be impacted by local natural precursor emissions, distant natural emissions, distant anthropogenic emissions, downwind transport processes, photochemical conditions, and terrain conditions including deposition with respect to forest or agricultural areas (Altshuller and Lefohn 1996; Chan et al., 2010; HTAP, 2010). Baseline O<sub>3</sub> can also be influenced by stratospheric intrusion (e.g., Altshuller and Lefohn 1996; Schroeder et al., 2014). Thus, it was expected that baseline CO and O<sub>3</sub> would not be identical between the seven sites due to the varying meteorology, terrain, elevation (18 – 2100 m asl), and land surface (marine to mountain top) at the sites. MWO and WFM are the two highest sites situated close to the top of the daytime convective boundary layer and they are likely more impacted by long-range transport and stratospheric intrusion. PSP is located either on the periphery of the subtropical high in summer – fall, or the periphery of the North American trough (Figure. 5b–e). Thus, PSP could be less influenced by the westerly wind. TF, which is close to the northeast urban corridor, could be more influenced by downwind transport from urban areas.

We explicitly discussed differences of baseline CO and O<sub>3</sub> among each site in Sections 3.2 – 3.3. Those differences among each site also help to identify the impact of increasing Asian emissions, NO<sub>x</sub> emissions from the northeast urban corridor, and stratospheric intrusion over the Northeast

US. In addition, similarities and differences of baseline CO and O<sub>3</sub> derived from our study illustrated the range of baseline CO and O<sub>3</sub> over the Northeast US.

To better compare similarities and differences between the seven sites, we reorganized the time series in Figure 2 by separating the time series at the two mountainous sites MWO and WFM, from the other five lower elevation sites.

3) It is clear that there are experimental problems in the data set. In the discussion the authors note unexplained differences between results at different sites. Some of these are certainly due to experimental problems. Before, proceeding with any attempt to define a regional concentration, the authors must undertake a critical evaluation of their data sets to eliminate confounding experimental problems.

It is not clear to us what exactly those “unexplained differences” the reviewer referred to. As we stated in our response to the reviewer’s Comment #2, we devoted Sections 3.2 – 3.3 to understanding the differences in baseline CO and O<sub>3</sub> between the sites. One unexplained difference we readily acknowledge is the unusually high CO mixing ratios at CS over May 2003 – June 2008. However, no evidence shows the causes for these high mixing ratios and suggests any experimental errors. We removed all the statements involving baseline CO at CS, and none of the conclusions was drawn based on this dataset. All other differences between sites were investigated and attributed to meaningful processes.

The data at five sites were obtained from the University of New Hampshire’s AIRMAP Observing Network (<http://www.eos.unh.edu/observatories/data.shtml>), a NOAA funded regional climate and air quality program. Since 1999, the AIRMAP program has conducted a wide range of measurements of chemical species, including O<sub>3</sub>, NO, NO<sub>y</sub>, CO, CO<sub>2</sub>, SO<sub>2</sub>, elemental mercury (Hg<sup>0</sup>), reactive gaseous mercury (RGM), particle-bound mercury (HgP), hydrocarbons, halocarbons, and oxygenated compounds. All of these measurements have undergone rigorous quality control, and many papers using these datasets have been published in peer reviewed journals over the years. The publications covered various topics, such as synoptic controls on Northeast surface O<sub>3</sub>, complex cycling of atmospheric mercury in terrestrial and coastal marine environments, and the distribution of hydrocarbons and halocarbons along coastal New England (e.g., Feddersen et al., 2012; Fischer and Talbot, 2005; Hegarty et al., 2007; Lai et al., 2012; Lombard et al., 2011; Mao et al., 2008; Mao and Talbot, 2004a, 2004b, 2004c, 2012; Sigler et al., 2009a, 2009b; Talbot et al., 2005, 2011). Specifically, CO was measured with Thermo Environmental Instruments model 48CTL. As the instrument baseline drifts constantly, it was operated in a mode where ambient air was monitored for 10 min followed by a 5-min zeroing interval. Zeroing was generating by converting CO to CO<sub>2</sub> using a hot (250 °C) palladium catalyst. Calibration was performed every 6.25 hours and it was conducted by providing a spike of 300 ppbv, which was dynamically diluted from ~5 ppmv (NIST traceable ±2%) CO standard from Scott Marrin, Inc. (Mao and Talbot, 2004). O<sub>3</sub> was measured using a Thermo Environmental Instruments model 49C-PS. The detection limit of the instrument was 1.0

ppbv. Instrument zeroing and calibration was achieved routinely by utilizing zeroing air and an internal primary O<sub>3</sub> source, respectively. In addition, TF was a part of AMNet over January 1, 2009 – November 29, 2011.

The dataset at WFM and PSP were obtained from the State University of New York at Albany. The Atmospheric Sciences Research Center at University at Albany (ASRC), in collaboration with New York State Department of Environmental Conservation (NYSDEC), has maintained and operated these measurement sites for decades. All the data have been quality controlled with the strictest protocols. The ASRC supersite dataset has been used for numerous peer-reviewed publications over the past decade. They have been used to evaluate air quality models, characterize the process leading to the formation of ozone and PM<sub>2.5</sub>, evaluate the regional impact of wildfires (e.g., Bae et al., 2011; Cai et al., 2008; Ren et al., 2003, 2006; Schwab et al., 2009).

We added a concise description including such information in the text (L214).

The correlations related to baseline CO at CS were deleted in Table 3 and Table 4. The statement “CS was not included, as mixing ratios of baseline CO at this site were unusually high over May 2003 – June 2008.” was added in Table 3 and Table 4. “CS,” was deleted in L570.

**4) Pages 27263-27280 give an extended discussion of many topics. Much of this discussion is speculation regarding causes of trends, variability and correlation perceived in the data. For a useful paper to eventually arise from the authors' analysis, the speculation must be removed, and clear, well-reasoned discussion must be substituted. I suggest that the authors focus on a limited set of hypotheses that they feel they can discuss in a rigorous and complete manner.**

The analysis on pages 27263-27280 resulted in the following findings:

1. Baseline CO at most sites decreased significantly at a rate between  $-4.3$  to  $-2.3$  ppbv yr<sup>-1</sup>, while baseline O<sub>3</sub> was relatively constant;
2. Springtime and wintertime baseline CO at MWO and WFM did not exhibit a significant trend, possibly a result of the combined effect of decreasing emissions in the northeast US and increasing emissions in Asia;
3. Increasing springtime and wintertime baseline O<sub>3</sub> at TF was most likely caused by the decrease in NO<sub>x</sub> emissions over the urban corridor;
4. Summertime baseline CO and O<sub>3</sub> were predominantly influenced by biomass burning emissions and cyclone activities, which were related to the AO;
5. Negative correlation was found between baseline O<sub>3</sub> and the NAO index, potentially due to variations of solar flux, stratospheric intrusion, and continental export.

To arrive at each finding, we used detail-oriented quantitative analysis, logical discussion of our own results, and the findings from the literature. A case in point is Finding #3, for which we initially had four hypotheses, and after carefully examining the dataset of potential vorticity, the difference among sites with different elevation, and O<sub>3</sub> photochemistry in combination with

findings from previous studies (e.g., Cooper et al., 2012; Reidmiller et al., 2009; Wilson et al., 2012), we arrived at the point that decreasing NO<sub>x</sub> emissions over the northeast urban corridor was the most probable factor contributing to increasing wintertime and springtime baseline O<sub>3</sub> at TF.

### Minor issues:

1) Figure 2 is confusing. The station labels in the annotations are not in accord with the figure caption. It is not clear which curve corresponds to which station.

Thanks for pointing out the mistake. Originally, Figures 2b and 2d showed time series of baseline CO and O<sub>3</sub> at WFM and PSP. We reorganized Figure 2, and in the new figure time series of baseline CO and O<sub>3</sub> at MWO and WFM were shown in Figure 2b and 2d.

### References

- Altshuller, a P.: Estimation of the natural background of ozone present at surface rural locations., *Japca*, 37(12), 1409–1417, doi:10.1080/08940630.1987.10466335, 1987.
- Altshuller, a. P. and Lefohn, A. S.: Background Ozone in the Planetary Boundary Layer Over the United States, *J. Air Waste Manag. Assoc.*, 46(2), 134–141, doi:10.1080/10473289.1996.10467445, 1996.
- Bae, M. S., Schwab, J. J., Chen, W. N., Lin, C. Y., Rattigan, O. V. and Demerjian, K. L.: Identifying pollutant source directions using multiple analysis methods at a rural location in New York, *Atmos. Environ.*, 45(15), 2531–2540, doi:10.1016/j.atmosenv.2011.02.020, 2011.
- Cai, C., Hogrefe, C., Katsafados, P., Kallos, G., Beauharnois, M., Schwab, J. J., Ren, X., Brune, W. H., Zhou, X., He, Y. and Demerjian, K. L.: Performance evaluation of an air quality forecast modeling system for a summer and winter season - Photochemical oxidants and their precursors, *Atmos. Environ.*, 42(37), 8585–8599, doi:10.1016/j.atmosenv.2008.08.029, 2008.
- Chan, E. and Vet, R. J.: Baseline levels and trends of ground level ozone in Canada and the United States, *Atmospheric Chem. Phys.*, 10(18), 8629–8647, doi:10.5194/acp-10-8629-2010, 2010.
- Cooper, O. R., Parrish, D. D., Stohl, a, Trainer, M., Nédélec, P., Thouret, V., Cammas, J. P., Oltmans, S. J., Johnson, B. J., Tarasick, D., Leblanc, T., McDermid, I. S., Jaffe, D., Gao, R., Stith, J., Ryerson, T., Aikin, K., Campos, T., Weinheimer, a and Avery, M. a: Increasing springtime ozone mixing ratios in the free troposphere over western North America., *Nature*, 463(7279), 344–348, doi:10.1038/nature08708, 2010.



Cooper, O. R., Gao, R. S., Tarasick, D., Leblanc, T. and Sweeney, C.: Long-term ozone trends at rural ozone monitoring sites across the United States, 1990-2010, *J. Geophys. Res. Atmospheres*, 117(22), 1990–2010, doi:10.1029/2012JD018261, 2012.

Cui, J., Pandey Deolal, S., Sprenger, M., Henne, S., Staehelin, J., Steinbacher, M. and Nédélec, P.: Free tropospheric ozone changes over Europe as observed at Jungfraujoch (1990-2008): An analysis based on backward trajectories, *J. Geophys. Res. Atmospheres*, 116(10), 1–14, doi:10.1029/2010JD015154, 2011.

Derwent, R. G., Simmonds, P. G., Manning, a. J. and Spain, T. G.: Trends over a 20-year period from 1987 to 2007 in surface ozone at the atmospheric research station, Mace Head, Ireland, *Atmos. Environ.*, 41(39), 9091–9098, doi:10.1016/j.atmosenv.2007.08.008, 2007.

Feddersen, D. M., Talbot, R., Mao, H. and Sive, B. C.: Size distribution of particulate mercury in marine and coastal atmospheres, *Atmospheric Chem. Phys.*, 12(22), 10899–10909, doi:10.5194/acp-12-10899-2012, 2012.

Fiore, A. M., Jacob, D. J., Bey, I., Yantosca, R. M., Field, B. D., Fusco, A. C. and Wilkinson, J. G.: Background ozone over the United States in summer: Origin, trend, and contribution to pollution episodes, *J. Geophys. Res. Atmospheres*, 107(D15), ACH 11–1, doi:10.1029/2001JD000982, 2002.

Fischer, E. and Talbot, R.: Regional NO<sub>3</sub>– events in the northeastern United States related to seasonal climate anomalies, *Geophys. Res. Lett.*, 32(16), L16804, doi:10.1029/2005GL023490, 2005.

Hegarty, J., Mao, H. and Talbot, R.: Synoptic controls on summertime surface ozone in the northeastern United States, *J. Geophys. Res. Atmospheres*, 112(D14), D14306, doi:10.1029/2006JD008170, 2007.

HTAP, H.: Hemispheric Transport of 2010 Part a : Ozone and Particulate Matter., 2010.

Huang, M., Bowman, K. W., Carmichael, G. R., Lee, M., Chai, T., Spak, S. N., Henze, D. K., Darmenov, A. S. and da Silva, A. M.: Improved western U.S. background ozone estimates via constraining nonlocal and local source contributions using Aura TES and OMI observations, *J. Geophys. Res. Atmospheres*, 120(8), 2014JD022993, doi:10.1002/2014JD022993, 2015.

Jaffe, D., Price, H., Parrish, D., Goldstein, A. and Harris, J.: Increasing background ozone during spring on the west coast of North America, *Geophys. Res. Lett.*, 30(12), 1613, doi:10.1029/2003GL017024, 2003.

Lai, T. L., Talbot, R. and Mao, H.: An investigation of two highest ozone episodes during the last decade in New England, *Atmosphere*, 3(1), 59–86, doi:10.3390/atmos3010059, 2012.

Lin, C.-Y. C., Jacob, D. J., Munger, J. W. and Fiore, A. M.: Increasing background ozone in surface air over the United States, *Geophys. Res. Lett.*, 27(21), 3465–3468, doi:10.1029/2000GL011762, 2000.

- Logan, J. a., Staehelin, J., Megretskaia, I. a., Cammas, J. P., Thouret, V., Claude, H., De Backer, H., Steinbacher, M., Scheel, H. E., Stbi, R., Frhlich, M. and Derwent, R.: Changes in ozone over Europe: Analysis of ozone measurements from sondes, regular aircraft (MOZAIC) and alpine surface sites, *J. Geophys. Res. Atmospheres*, 117(9), 1–23, doi:10.1029/2011JD016952, 2012.
- Lombard, M. A. S., Bryce, J. G., Mao, H. and Talbot, R.: Mercury deposition in Southern New Hampshire, 2006-2009, *Atmospheric Chem. Phys.*, 11(15), 7657–7668, doi:10.5194/acp-11-7657-2011, 2011.
- Mao, H. and Talbot, R.: O<sub>3</sub> and CO in New England: Temporal variations and relationships, *J. Geophys. Res. Atmospheres*, 109(21), 1–19, doi:10.1029/2004JD004913, 2004a.
- Mao, H. and Talbot, R.: Relationship of surface O<sub>3</sub> to large-scale circulation patterns during two recent winters, *Geophys. Res. Lett.*, 31(6), L06108, doi:10.1029/2003GL018860, 2004b.
- Mao, H. and Talbot, R.: Role of meteorological processes in two New England ozone episodes during summer 2001, *J. Geophys. Res. Atmospheres*, 109(20), 1–17, doi:10.1029/2004JD004850, 2004c.
- Mao, H. and Talbot, R.: Speciated mercury at marine, coastal, and inland sites in New England- Part 1: Temporal variability, *Atmospheric Chem. Phys.*, 12(11), 5099–5112, doi:10.5194/acp-12-5099-2012, 2012.
- Mao, H., Talbot, R. W., Sigler, J. M., Sive, B. C. and Hegarty, J. D.: Seasonal and diurnal variations of Hg<sup>o</sup> over New England, *Atmos Chem Phys*, 8(5), 1403–1421, doi:10.5194/acp-8-1403-2008, 2008.
- Parrish, D. D., Millet, D. B. and Goldstein, A. H.: Increasing ozone in marine boundary layer inflow at the west coasts of North America and Europe, *Atmospheric Chem. Phys.*, 9(4), 1303–1323, 2009.
- Parrish, D. D., Aikin, K. C., Oltmans, S. J., Johnson, B. J., Ives, M. and Sweeny, C.: Impact of transported background ozone inflow on summertime air quality in a California ozone exceedance area, *Atmospheric Chem. Phys.*, 10(20), 10093–10109, doi:10.5194/acp-10-10093-2010, 2010.
- Parrish, D. D., Law, K. S., Staehelin, J., Derwent, R., Cooper, O. R., Tanimoto, H., Volz-Thomas, a., Gilge, S., Scheel, H. E., Steinbacher, M. and Chan, E.: Long-term changes in lower tropospheric baseline ozone concentrations at northern mid-latitudes, *Atmospheric Chem. Phys.*, 12(23), 11485–11504, doi:10.5194/acp-12-11485-2012, 2012.
- Reidmiller, D. R., Jaffe, D. a., Chand, D., Strode, S., Swartzendruber, P., Wolfe, G. M. and Thornton, J. a.: Interannual variability of long-range transport as seen at the Mt. Bachelor Observatory, *Atmospheric Chem. Phys. Discuss.*, 8(4), 16335–16379, doi:10.5194/acpd-8-16335-2008, 2009.
- Ren, X., Harder, H., Martinez, M., Leshner, R. L., Oligier, A., Simpas, J. B., Brune, W. H., Schwab, J. J., Demerjian, K. L., He, Y., Zhou, X. and Gao, H.: OH and HO<sub>2</sub> chemistry in the

urban atmosphere of New York City, *Atmos. Environ.*, 37(26), 3639–3651, doi:10.1016/S1352-2310(03)00459-X, 2003.

Ren, X., Brune, W. H., Olinger, A., Metcalf, A. R., Simpas, J. B., Shirley, T., Schwab, J. J., Bai, C., Roychowdhury, U., Li, Y., Cai, C., Demerjian, K. L., He, Y., Zhou, X., Gao, H. and Hou, J.: OH, HO<sub>2</sub>, and OH reactivity during the PMTACS-NY Whiteface Mountain 2002 campaign: Observations and model comparison, *J. Geophys. Res. Atmospheres*, 111(10), doi:10.1029/2005JD006126, 2006.

Schroeder, J. R., Pan, L. L., Ryerson, T., Diskin, G., Hair, J., Meinardi, S., Simpson, I., Barletta, B., Blake, N. and Blake, D. R.: Evidence of mixing between polluted convective outflow and stratospheric air in the upper troposphere during DC3, *J. Geophys. Res. Atmospheres*, 119(19), 2014JD022109, doi:10.1002/2014JD022109, 2014.

Schwab, J. J., Spicer, J. B. and Demerjian, K. L.: Ozone, trace gas, and particulate matter measurements at a rural site in southwestern New York state: 1995–2005, *J. Air Waste Manag. Assoc.* 1995, 59(3), 293–309, 2009.

Sigler, J. M., Mao, H. and Talbot, R.: Gaseous elemental and reactive mercury in Southern New Hampshire, *Atmospheric Chem. Phys.*, 9(6), 1929–1942, 2009a.

Sigler, J. M., Mao, H., Sive, B. C. and Talbot, R.: Oceanic influence on atmospheric mercury at coastal and inland sites: A springtime nor'easter in New England, *Atmospheric Chem. Phys.*, 9(12), 4023–4030, 2009b.

Talbot, R., Mao, H. and Sive, B.: Diurnal characteristics of surface level O<sub>3</sub> and other important trace gases in New England, *J. Geophys. Res. Atmospheres*, 110(9), 1–16, doi:10.1029/2004JD005449, 2005.

Talbot, R., Mao, H., Feddersen, D., Smith, M., Kim, S. Y., Sive, B., Haase, K., Ambrose, J., Zhou, Y. and Russo, R.: Comparison of particulate mercury measured with manual and automated methods, *Atmosphere*, 2(1), 1–20, doi:10.3390/atmos2010001, 2011.

Wilson, R. C., Fleming, Z. L., Monks, P. S., Clain, G., Henne, S., Kononov, I. B., Szopa, S. and Menut, L.: Have primary emission reduction measures reduced ozone across Europe? An analysis of European rural background ozone trends 1996–2005, *Atmospheric Chem. Phys.*, 12(1), 437–454, doi:10.5194/acp-12-437-2012, 2012.

1 **Regional and Hemispheric Influences on Variability and Trends of Baseline**  
2 **Carbon Monoxide and Ozone over the Northeast US**~~Baseline—carbon~~  
3 **monoxide and ozone in the northeast US over 2001–2010**

4 **Y. Zhou<sup>1</sup>, H. Mao<sup>1</sup>, K. Demerjian<sup>2</sup>, C. Hogrefe<sup>3</sup>, and J. Liu<sup>4,5</sup>**

5 <sup>1</sup> Department of Chemistry, State University of New York College of Environmental Science and  
6 Forestry, Syracuse, NY 13210, USA

7 <sup>2</sup> Atmospheric Science Research Center, State University of New York at Albany, Albany, NY  
8 12203, USA

9 <sup>3</sup> Emissions and Model Evaluation Branch, Atmospheric Modeling and Analysis Division,  
10 NERL, ORD, U.S. EPA, Research Triangle Park, NC 27711, USA

11 <sup>4</sup> School of Atmospheric Sciences, Nanjing University, Nanjing, 210093, China

12 <sup>5</sup> Department of Geography and ~~Program in~~ Planning, University of Toronto, ~~100 St. George~~  
13 ~~Street~~, Toronto, ON M5S 3G3, Canada

14 Received: 17 August 2015 – Accepted: 5 September 2015 – Published: 8 October 2015

15 Correspondence to: Y. Zhou (yzhou51@syr.edu)

16 Published by Copernicus Publications on behalf of the European Geosciences Union.

17

18

19

20

21

22

23

24

25

26

27 **Abstract**

28 Baseline carbon monoxide (CO) and ozone (O<sub>3</sub>) were defined as mixing ratios of CO and O<sub>3</sub>  
29 under minimal influence of recent and local emissions. In this study, ~~Baseline~~-baseline carbon  
30 monoxide (CO) and ozone (O<sub>3</sub>) were ~~examined~~studied at seven rural sites in the northeast US  
31 during varying periods over 2001–2010. ~~Specifically, baseline air was determined using the~~  
32 monthly 10<sup>th</sup> percentile level of CO at Appledore Island (AI), Castle Spring (CS), Pack  
33 Monadnock (PM), Thompson Farm (TF), Pinnacle State Park (PSP), and 50<sup>th</sup> percentile level at  
34 Mt. Washington (MWO) and Whiteface Mountain (WFM). Monthly median O<sub>3</sub> levels of the  
35 baseline air were defined as baseline O<sub>3</sub> levels. Interannual and seasonal variations of baseline  
36 CO and O<sub>3</sub> were examined for the effects of changes in anthropogenic emissions, stratospheric  
37 intrusion, transport pathways and O<sub>3</sub> photochemistry. Baseline CO generally exhibited  
38 decreasing trends at most sites, except at ~~Castle Spring (CS)~~, an elevated (~ 400 ma.s.l.) site in  
39 rural central New Hampshire. Over April 2001–December 2010, baseline CO at ~~Thompson Farm~~  
40 ~~(TF)~~, ~~Pinnacle State Park (PSP)~~, and ~~Whiteface Mountain (WFM)~~ decreased at rates ranging  
41 from -4.3 to -2.5 ppbv yr<sup>-1</sup>. Baseline CO decreased significantly at a rate of -2.3 ppbv yr<sup>-1</sup> at  
42 ~~Mt. Washington (MWO)~~ over April 2001–March 2009, and -3.5 ppbv yr<sup>-1</sup> at ~~Pack Monadnock~~  
43 ~~(PM)~~ over July 2004–October 2010. Unlike baseline CO, baseline O<sub>3</sub> did not display a  
44 significant long term trend at any of the sites, resulting probably from opposite trends in NO<sub>x</sub>  
45 emissions worldwide and possibly from the overall relatively constant mixing ratios of CH<sub>4</sub> in  
46 the 2000s. In looking into long term trends by season, wintertime baseline CO at MWO and  
47 WFM, the highest sites, did not exhibit a significant trend, probably due to the competing effects  
48 of decreasing CO emissions in the US and increasing emissions in Asia. Springtime and  
49 wintertime baseline O<sub>3</sub> at TF increased significantly at a rate of 2.4 and 2.7 ppbv yr<sup>-1</sup>,

50 respectively, which was likely linked to nitrogen oxides ( $\text{NO}_x$ ) emissions reductions over urban  
51 areas and possible resultant increases in  $\text{O}_3$  due to less titration by NO in urban plumes. The  
52 effects of meteorology on baseline  $\text{O}_3$  and CO were investigated. A negative correlation was  
53 found between springtime baseline  $\text{O}_3$  and the North Atlantic oscillation (NAO) index. It was  
54 found that during positive NAO years, lower baseline  $\text{O}_3$  in the northeast US was linked to less  
55 solar radiation flux, weakened stratospheric intrusion, and intensified continental export. The  
56 lowest baseline CO at ~~Appledore Island (AI)~~, PM, TF, PSP, WFM and the lowest baseline  $\text{O}_3$  at  
57 AI, PM, and PSP in summer 2009 were linked to the negative phase of the Arctic oscillation  
58 (AO), when more frequent cyclone activities brought more clean Arctic air to midlatitudes. It  
59 was also found that forest fires played a major role in determining baseline CO in the northeast  
60 US over 2001–2010. In summer, ~ 38 % of baseline CO variability at AI, CS, MWO, TF, PSP,  
61 and WFM could be explained by CO emissions from forest fires in Russia and ~ 22 % by  
62 emissions from forest fires in Canada. Long-range transport of  $\text{O}_3$  and its precursors from  
63 biomass burning contributed to the highest baseline  $\text{O}_3$  in summer 2003 at AI, CS, MWO, TF,  
64 and WFM. The findings of this study suggested impacts of increasing Asian emissions,  $\text{NO}_x$   
65 emissions from the Northeast Urban corridor, global biomass burning emissions, and  
66 meteorological conditions (e.g. cyclone activity, AO, and NAO) should all be considered when  
67 designing strategies for meeting and maintaining National Ambient Air Quality Standards  
68 (NAAQS) and evaluating the air quality in the northeast US.

69

70

71

72

## 1 Introduction

Carbon monoxide (CO) is a product of incomplete combustion (e.g. fossil fuel, biofuel, and biomass burning) and oxidation of hydrocarbon compounds (Worden et al., 2013). CO is a major sink of hydroxyl radicals (OH), and hence changes in CO can impact many chemically important trace species that are removed via oxidation by OH (Daniel and Solomon, 1998; Petrenko et al., 2013). In the presence of nitrogen oxides (NO<sub>x</sub>), CO oxidation is important in the tropospheric ozone (O<sub>3</sub>) budget. Due to its relatively unreactive chemical nature, CO has been used as a tracer of anthropogenic influence and fire emissions (Gratz et al., 2014; Price et al., 2004; Weiss-Penzias et al., 2006).

Tropospheric ~~ozone (O<sub>3</sub>)~~, which is produced largely by photochemical oxidation of ~~nitrogen oxides (NO<sub>x</sub>)~~ and volatile organic compounds (VOCs), is a serious and ubiquitous air pollutant affecting humans' respiratory system, reducing yields of agricultural crops, and damaging natural ecosystems (EPA, 2012). As a precursor of ~~hydroxyl radicals (OH)~~, a dominant oxidant, O<sub>3</sub> regulates the atmospheric capacity of oxidation (Prinn, 2003). Tropospheric O<sub>3</sub> is also the third strongest greenhouse gas, after carbon dioxide (CO<sub>2</sub>) and methane (CH<sub>4</sub>), suggested by the Intergovernmental Panel on Climate Change (IPCC, 2007).

~~CO is a product of incomplete combustion (e.g. fossil fuel, biofuel, and biomass burning) and oxidation of hydrocarbon compounds (Worden et al., 2013). CO is a major sink of OH, and hence changes in CO can impact many chemically important trace species that are removed via oxidation by OH (Daniel and Solomon, 1998; Petrenko et al., 2013). In the presence of NO<sub>x</sub>, CO oxidation is important in the tropospheric O<sub>3</sub> budget. Due to its relatively unreactive chemical nature, CO has been used as a tracer of anthropogenic influence and fire emissions (Gratz et al., 2014; Price et al., 2004; Weiss-Penzias et al., 2006).~~

96 The United States has made enormous efforts to control ambient mixing ratios of criteria  
97 pollutants since the 1970s (EPA, 2012). Nationally, annual second maximum 8 h average mixing  
98 ratios of CO decreased by 52 %, and annual mean mixing ratios of nitrogen dioxide (NO<sub>2</sub>)  
99 declined by 33 % over 2001–2010 (EPA, 2012). Ambient O<sub>3</sub> concentrations in metropolitan  
100 areas, such as Los Angeles, New York City, and Chicago, decreased significantly in the past two  
101 decades (Bell et al., 2007; Cooper et al., 2010, 2012; Lefohn et al., 2010; Parrish et al., 2011).  
102 Despite the decreasing anthropogenic emissions in Europe and North America, emissions in  
103 China and India have increased. Biomass burning emissions vary both spatially and temporally  
104 (Granier et al., 2011; Gratz et al., 2014). It remains unclear how such opposing changes in  
105 emissions have globally affected baseline CO and O<sub>3</sub>, which are defined as mixing ratios of CO  
106 and O<sub>3</sub> under minimal influence of recent and local emissions (Chan and Vet, 2010; HTAP,  
107 2010).

108 Background or baseline has been used, often interchangeably, to quantify how much O<sub>3</sub>  
109 produced from recent or local anthropogenic emissions could be allowed to attain the O<sub>3</sub>  
110 standards (HTAP, 2010; Huang et al., 2015). A few recent studies discussed the difference  
111 between background O<sub>3</sub> and baseline O<sub>3</sub> (HTAP, 2010; Huang et al., 2015; Parrish et al., 2012;  
112 Chan et al., 2010). The term “background” was used in modeling studies that estimated the  
113 atmospheric mixing ratio of a compound determined by natural sources only, while the term  
114 “baseline” was obtained from measurement records by removing data of local influences (HTAP,  
115 2010, Chan et al., 2010; Parrish et al., 2012). Quantitative estimates of baseline CO and O<sub>3</sub> are  
116 not straightforward since measurements at a particular location include contributions from local  
117 anthropogenic precursor emissions (Chan and Vet, 2010). Various methods have been utilized to  
118 diagnose baseline conditions, including using measurements at remote sites, analysis of the



119 probability distribution of pollutants, correlations with reactive nitrogen oxides, and isentropic  
120 back-trajectories (e.g., Altshuller and Lefohn, 1996; Lin et al., 2000; Jaffe et al., 2003; Derwent  
121 et al., 2007; Parrish et al., 2009; Cui et al., 2011; Wilson et al., 2012). ~~In the literature, Air~~  
122 masses with low percentile values (< 20th percentile in the literature) of CO, an excellent  
123 anthropogenic tracer for its origin of mobile combustion, are commonly considered background  
124 baseline air (e.g., Lin et al., 2000; Mao and Talbot, 2012). Based on Lin et al. (2000), ~~t~~The low  
125 percentile value of CO is used as baseline CO, and baseline O<sub>3</sub> is then estimated using the data  
126 corresponding to CO mixing ratios below the baseline CO level ~~(e.g., Lin et al., 2000; Mao and~~  
127 ~~Talbot, 2012).~~

128         The lifetime of CO and O<sub>3</sub> in the free troposphere is ~ 2 months and ~ 20 days,  
129 respectively (Price et al., 2004; Stevenson et al., 2006). Thus, CO, O<sub>3</sub>, and other precursors  
130 emitted in the upwind region and those produced in transit could affect the baseline CO and O<sub>3</sub>  
131 levels there~~be transported downwind and subsequently affect the baseline CO and O<sub>3</sub> levels there~~  
132 (Cooper et al., 2012; Oltmans et al., 2008; Pollack et al., 2013). This has important regulatory  
133 implications, because the levels of baseline CO and O<sub>3</sub> directly affect emission control of CO  
134 and other O<sub>3</sub> precursors. Therefore, quantifying trends and variations in baseline CO and O<sub>3</sub> is of  
135 vital importance to assessing air quality and designing cost-effective emission control plans to  
136 meet the National Ambient Air Quality Standards (NAAQS)  
137 (<http://www3.epa.gov/ttn/naaqs/criteria.html>).

138         Studies have been conducted to investigate trends in baseline CO and O<sub>3</sub> across northern  
139 hemispheric mid-latitudes regions, such as North America, Europe, and Asia, and no consistent  
140 trends have been found (Chan, 2009; Cooper et al., 2010; Cui et al., 2011; Logan et al., 2012;  
141 Oltmans et al., 2013; Parrish et al., 2012; Tilmes et al., 2012; Wilson et al., 2012; Xu et al.,

142 | 2008). ~~No consistent trends have been found.~~ Kumar et al. (2013) reported trends of  $-0.31$  and  
143  $-0.21$  ppbv  $\text{yr}^{-1}$  for CO and O<sub>3</sub>, respectively, at the Pico Mountain Observatory over 2001–2011.  
144 Gratz et al. (2014) reported that the springtime median mixing ratio of O<sub>3</sub> increased at a rate of  
145  $0.76$  ppbv  $\text{yr}^{-1}$  at the Mt. Bachelor Observatory over 2004–2013, while median CO decreased at  
146 a rate of  $-3.1$  ppbv  $\text{yr}^{-1}$ . Chan and Vet (2010) found that baseline O<sub>3</sub> in the eastern US decreased  
147 in spring, summer, and fall over 1997–2006, and the decadal trends in the Atlantic coastal region  
148 were positive in winter, summer, and fall. For the most part, causes for temporal variability have  
149 not been adequately explained. Interpretation of long-term trends is difficult because of  
150 significant interannual variability in emissions and climate as well as possibly in photochemistry  
151 (Hess and Lamarque, 2007). Climate change may lead to changes in natural emissions (e.g.,  
152 emissions from wildfires, vegetation, and lightning), pollution transport pathways, and  
153 stratosphere-tropospheric exchange (Parrish et al., 2013).

154 Wildfires release large quantities of O<sub>3</sub> precursors, e.g., CO, VOCs, and NO<sub>x</sub>, every year.  
155 For instance, the MACCity emission inventory over 2001–2010 suggested that total global  
156 biomass burning emissions of CO ranged from  $\sim 300$  to  $\sim 460$  Tg  $\text{yr}^{-1}$ , close to  $\sim 590$  Tg  $\text{yr}^{-1}$   
157 anthropogenic emissions (Granier et al., 2011). These chemical species could make a significant  
158 contribution to tropospheric CO and O<sub>3</sub> budgets, impacting the interannual variability of surface  
159 CO and O<sub>3</sub> globally (Dutkiewicz et al., 2011; Herron-Thorpe et al., 2014; Honrath et al., 2004;  
160 Kang et al., 2014; Wigder et al., 2013; Wotawa and Trainer, 2000). Most studies focused on  
161 episodic enhancements in demonstrated elevated CO and O<sub>3</sub> linked to due to fire emissions  
162 studies (e.g., DeBell et al., 2004; Dutkiewicz et al., 2011; Honrath et al., 2004) for an episode  
163 (Dutkiewicz et al., 2011; Honrath et al., 2004). To the best of our knowledge, only two studies  
164 (Jaffe et al., 2004; Wotawa et al., 2001) examined quantified the impact of wildfires on baseline

165 | CO and O<sub>3</sub> over time periods of ten years in the 1990s ~~using ten-year observations~~. Thus mMore  
166 | research is warranted to determine the impact of wildfires on baseline CO and O<sub>3</sub> in the 2000s in  
167 | northern hemispheric midlatitudes.

168 |       Regional climatic processes over the US east coast are influenced by the North Atlantic  
169 | Oscillation (NAO) and the Arctic Oscillation (AO) (Archambault et al., 2008; Hess and  
170 | Lamarque, 2007). Studies suggested a link between NAO and regional distributions of  
171 | tropospheric trace gases over the northwestern Atlantic Ocean, northern Europe, and the Arctic  
172 | region based on model simulations or measurements (Christoudias et al., 2012; Creilson et al.,  
173 | 2003; Duncan and Bey, 2004; Eckhardt et al., 2003; Hegarty et al., 2009; Krichak and Alpert,  
174 | 2005; Li et al., 2002; Pausata et al., 2012; Woollings and Blackburn, 2012). Most studies  
175 | suggested that trace gases over North America could be transported across the Atlantic Ocean to  
176 | northern Europe during the high NAO phase, particularly in winter and spring. However, to the  
177 | best of our knowledge, nearly no studies examined the relationship between NAO and trace  
178 | | gases over the northeast US over 2001 – 2010. Circulation patterns can not only impact the  
179 | transport of pollutants to the targeted region but can also influence the export from the upwind  
180 | region. Hence, upwind trace gases are also likely to change in response to varying intensity of  
181 | NAO.

182 |       The AO is another dominant mode of meteorological variability in the Northern  
183 | Hemisphere (Creilson et al., 2005; Hess and Lamarque, 2007; Pausata et al., 2012). AO is  
184 | characterized by winds circulating counterclockwise around the Arctic at around 55°N latitude,  
185 | (Thompson and Wallace, 2000). In a positive AO phase, surface pressure in the polar region is  
186 | abnormally low and strong winds around the pole confine cold air masses in the Arctic region;  
187 | | otherwise, more Arctic cold air dives south and increases storminess in the mid-latitudes regions

188 (Thompson and Wallace, 2000). Oswald et al. (2015) hypothesized that observed higher  
189 summertime O<sub>3</sub> levels in the northeast US was associated with less storminess in a positive AO  
190 phase. Some modeling studies suggested a weak impact from stratosphere-tropospheric exchange  
191 of O<sub>3</sub> on the lower troposphere over the Atlantic basin during a positive AO year (Brand et al.,  
192 2008; Hess and Lamarque, 2007; Lamarque and Hess, 2004). The impact of AO on surface O<sub>3</sub> in  
193 the northeast US needs to be further investigated using long-term surface measurement data.

194 Our study used long-term observations at seven rural sites in the Northeast US. Five are  
195 located in rural New Hampshire (NH) and two are in rural New York (NY) State. Although  
196 numerous studies have been conducted to understand the distributions of surface CO and O<sub>3</sub> in  
197 the northeast US and their controlling mechanisms (e.g. Bae et al., 2011; Hegarty et al., 2007<sup>9</sup>;  
198 Lai et al., 2012; Mao and Talbot, 2004; Schwab et al., 2009; Zhou et al., 2007), little work was  
199 done on baseline CO and O<sub>3</sub> using long-term measurement data for the region. Here, the trends  
200 of baseline CO and O<sub>3</sub> were examined at each site for the time period of 2001–2010, and  
201 regional to global emissions and large scale circulation patterns were investigated for their roles  
202 in the interannual and seasonal variation of baseline CO and O<sub>3</sub>.

## 203 **2 Methods and data**

### 204 **2.1 Measurement data**

205 The seven rural sites selected in this study (Table 1 and Fig. 1) are within a few hundred  
206 kilometers of each other. Their elevation varies between 18 and 2100 m. Measurements of CO,  
207 O<sub>3</sub>, wind direction, wind speed, and relative humidity at Appledore Island (AI), Castle Spring  
208 (CS), Mount Washington (MWO), Pack Monadnock (PM), and Thompson Farm (TF) were  
209 conducted by the University of New Hampshire (UNH) AIRMAP Observing Network  
210 (<http://www.eos.unh.edu/observatories/data.shtml>). The time resolution of the continuous year-

211 round measurements at these five sites was one minute. At AI, CO was measured seasonally  
212 from May to September over 2001–2006 and year round over 2007–2011, and O<sub>3</sub> was measured  
213 seasonally from May to September over 2002–2007 and year-round over 2008–2011. All of the  
214 measurements have undergone rigorous quality controls and tThe description of CO and O<sub>3</sub>  
215 measurement techniques from the UNH AIRMAP sites can be found in Mao and Talbot (2004).  
216 Additionally, hourly data of solar radiation flux were available at TF over January 2002–  
217 December 2010 from the Climate Reference Network (CRN) run by the National Ocean and  
218 Atmospheric Administration (NOAA) (<http://www.ncdc.noaa.gov/crn/data-access>). The one-  
219 hour measurement data of CO, O<sub>3</sub>, wind direction, wind speed, and relative humidity at  
220 Whiteface Mountain (WFM) and Pinnacle State Park (PSP) began around 1996 (Table 1). The  
221 description of CO and O<sub>3</sub> measurement techniques for WFM and PSP can be found in Brandt et  
222 al. (2015) and Schwab et al. (2009). The time in all of the datasets was expressed in coordinated  
223 universal time (UTC), i.e. local time +5 h for non-daylight saving time and +4 h for daylight  
224 saving time (March–November).

## 225 **2.2 Quantification of baseline CO and O<sub>3</sub>**

226 The local afternoon time window (18:00–24:00 UTC) was selected to avoid including the  
227 data representing nighttime depletion of O<sub>3</sub> due to dry deposition and titration (Talbot et al.,  
228 2005). The planetary boundary layer (PBL) is well mixed in the afternoon. The monthly 10th  
229 percentile mixing ratio of CO at AI, CS, PM, TF, and PSP was used to represent the baseline CO  
230 levels. As MWO and WFM are located atop the mountains, they are far less impacted by local  
231 anthropogenic emissions. Therefore, monthly median values of CO were selected at MWO and  
232 WFM to represent the baseline level. To determine baseline O<sub>3</sub> levels, we first created a subset of  
233 O<sub>3</sub> data by using the O<sub>3</sub> mixing ratios corresponding to CO mixing ratios below the monthly 10th

234 percentile values at AI, CS, PM, TF, and PSP and monthly median values at MWO and WFM.  
235 The monthly median values of this subset were then defined as the baseline O<sub>3</sub> levels for  
236 respective sites.

### 237 **2.3 Datasets**

238 The NAO index is a measure of the intensity of NAO, which is defined based on the leading  
239 empirical orthogonal function of the normalized sea level pressure difference between the  
240 subtropical high and the subpolar low using the National Centers for Environmental  
241 Prediction/National Center for Atmospheric Research (NCEP/NCAR) reanalysis (Barnston and  
242 Livezey, 1987). The AO index was obtained by projecting the daily 1000 hPa geopotential height  
243 anomalies poleward of 20°N onto the loading pattern of the AO (Thompson and Wallace, 2000).  
244 The Climate Prediction Center of NCEP ([http://www.cpc.ncep.noaa.gov/data/teledoc/  
245 telecontents.shtml](http://www.cpc.ncep.noaa.gov/data/teledoc/telecontents.shtml)) routinely monitors the primary teleconnection patterns. Monthly climate  
246 index values of NAO and AO were used in this study to understand the roles of global transport  
247 of atmospheric species via large-scale atmospheric circulation.

248 The Global Fire Emission Data (GFED) combines satellite information of fire activities  
249 and vegetation productivities, and contains the gridded monthly burned area and fire emissions.  
250 GFED 3 (<http://www.globalfiredata.org/>) was used in this study to estimate the biomass burning  
251 emissions of CO over Russia, Canada, California, and Alaska. Data were available for 2001–  
252 2010 at 0.5° × 0.5° horizontal resolution. Monthly mean global CO columns with 1° × 1° resolution  
253 obtained from the Measurements of Pollution in the Troposphere (MOPITT) instrument on the  
254 satellite Terra (<https://www2.acd.ucar.edu/mopitt/>) were used for the time period of 2001–2010  
255 over grids containing Russia, Canada, Alaska, and California, when wildfire CO emissions in  
256 these grids calculated from GFED were larger than 1 g m<sup>-2</sup> month<sup>-1</sup>.

257 Monthly wind, geopotential height, temperature, relative humidity ([http://www.esrl.noaa.](http://www.esrl.noaa.gov/psd/data/gridded/data.ncep.reanalysis.html)  
258 [gov/psd/data/gridded/data.ncep.reanalysis.html](http://www.esrl.noaa.gov/psd/data/gridded/data.ncep.reanalysis.html)), and potential vorticity (PV) ([http://rda.ucar.edu/](http://rda.ucar.edu/datasets/ds090.0)  
259 [datasets/ds090.0](http://rda.ucar.edu/datasets/ds090.0)) with a spatial resolution of  $2.5^{\circ} \times 2.5^{\circ}$  from the NCEP/NCAR Global Reanalysis  
260 Products were used for meteorological conditions and for identifying stratospheric intrusion.

261 The dataset representing  $O_3$  of stratospheric origin, constructed by Liu et al. (2013)  
262 (<ftp://es-ee.tor.ec.gc.ca/pub/ftpdt/Stratospheric%20Climatology/>), was also used to verify the  
263 contribution of stratospheric  $O_3$  to the two mountain sites and the decadal trends there. This  
264 dataset included monthly amounts of stratospheric  $O_3$  from the surface to 26 km altitude with  $5^{\circ} \times$   
265  $5^{\circ} \times 1$  km spatial resolution from the 1960s to the 2000s.

266 Mean sea level pressure data were obtained from NCEP-DOE Reanalysis 2  
267 (<http://www.esrl.noaa.gov/psd/data/gridded/data.ncep.reanalysis2.html>). The dataset is six hourly  
268 with a spatial resolution of  $2.5^{\circ} \times 2.5^{\circ}$ . The data were used to identify and quantify the cyclones  
269 that passed over the northeast US.

#### 270 **2.4 Mid-latitude cyclone identification and tracking**

271 Many algorithms have been developed since the 1970s to identify mid-latitude cyclones  
272 (Hu et al., 2004; Murazaki and Hess, 2006; Racherla and Adams, 2008). The algorithm  
273 developed by Bauer and Del Genio (2006) was adopted in this study to track the sea level  
274 pressure minima. The first step of the algorithm was to search for the local minimum by a 2 grids  
275  $\times$  2 grids matrix. The next step was to search for the local (within 720 km) minimum in the next  
276 6 h time step, assuming that a cyclone cannot move faster than  $120 \text{ km h}^{-1}$ , the same criterion  
277 used by Bauer and Del Genio (2006). If more than one local minimum was found, the point with  
278 the lowest sea level pressure was designated as the center of a cyclone.~~the center of a cyclone~~  
279 ~~was obtained.~~ Two more criteria were applied, its duration  $> 24$  h and central pressure  $\leq 1020$

280 hPa. Long-term cyclone frequency statistics were calculated for the northeast US (37.5–47.5°N,  
281 67.5–82.5°W).

## 282 **2.5 Statistical methods**

283 The open-air package in the statistical programming language R 3.0.2 was used to  
284 determine whether a rate of change was statistically significant. Trends in baseline CO and O<sub>3</sub>  
285 were reported using SenTheil slopes from the non-parametric Mann–Kendall analysis in ppbv  
286 yr<sup>-1</sup> with 90 % confidence intervals. Pearson correlation was computed to determine the relation  
287 between variables (e.g. baseline CO, baseline O<sub>3</sub>, NAO index, relative humidity). The Student t  
288 test was conducted to verify statistical significance ( $\alpha = 0.10$ ).

289 To quantify the contribution to a location of interest from biomass burning emissions  
290 over an area, we applied the following linear regression models (Wotawa et al., 2001):

$$291 \quad \text{CO} = a_0 + a_1 E \quad (1)$$

292 Where CO is the mixing ratio of baseline CO at each site,  $E$  the total CO column over the area,  $a_0$   
293 the intercept value, and  $a_1$  the slope value. The combined effect of biomass burning emissions  
294 from Russia ( $E_{\text{Russia}}$ ) and Canada ( $E_{\text{Canada}}$ ) was computed using Eq. (2):

$$295 \quad \text{CO} = b_0 + b_1 E_{\text{Russia}} + b_2 E_{\text{Canada}} \quad (2)$$

296 where  $b_0$ ,  $b_1$ , and  $b_2$  are regression parameters. Note that  $E_{\text{Russia}}$  and  $E_{\text{Canada}}$  were found to be the  
297 two emissions sources that contributed significantly to the baseline CO at the seven sites of our  
298 study, which is why only these two sources were included in the regression.

## 299 **3 Results and discussions**

### 300 **3.1 General characteristics**

#### 301 **3.1.1 Baseline CO**



302 Baseline CO at CS, MWO, PM, TF, and PSP had maxima uniformly in March and  
303 minima in varying months over August–October (Fig. 2a and b). Averaged annual maxima were  
304 191 ppbv at CS, 180 ppbv at MWO, 155 ppbv at PM, 164 ppbv at TF, and 189 ppbv at PSP over  
305 their respective time periods (Table 1). Averaged annual minima were 131 ppbv in August at CS,  
306 142 ppbv in September at MWO, 109 ppbv in October at PM, 113 ppbv in August at TF, and 128  
307 ppbv in October at PSP. At AI, year-round data were available during 2007–2010, a much  
308 shorter time period compared to those at other sites. The seasonal cycles at AI were consistent  
309 with other sites, with the average annual maximum 149 ppbv in March and minimum 103 ppbv  
310 in September. Previous studies suggested that the annual maximum in cold months resulted from  
311 residential heating, vehicle cold starts, and less loss from oxidation by OH, while the annual  
312 minimum in fall, instead of in June–July when solar radiation and hence OH concentrations  
313 reach annual maxima, was probably the combined effect of biomass burning emissions, mobile  
314 combustion emissions, and loss from oxidation by OH (Kopacz et al., 2010; Miller et al., 2008).

315 The annual cycle at WFM was different from those at all other sites, with an annual  
316 maximum of 144 ppbv in July and minimum of 103 ppbv in December averaged over January  
317 2001–December 2010 (Fig. 2b). To investigate the potential reasons for this different behavior,  
318 the data at WFM were compared with those at MWO, a site with slightly higher elevation (2 km  
319 a.s.l.) located 208 km to the east (Fig. 1). WFM and MWO are 128 km southwest and 217 km  
320 southeast, respectively, from Montreal, the 9th largest city in North America. Over 2001–2009,  
321 averaged summertime baseline CO (141 ppbv) at WFM was comparable to that (145 ppbv) at  
322 MWO, while averaged wintertime baseline CO (108 ppbv) at WFM was 60 ppbv or 36 % less  
323 than that (168 ppbv) at MWO (Fig. 2a and b). This wintertime contrast was probably associated  
324 with the large difference between the frequency distributions of wind direction at the two sites.

325 There were 4.7 % of the air masses at WFM from the northeast (22.5–67.5°), compared to 75.4 %  
326 of the air masses at MWO from the northwest (247.5–337.5°), the general direction of Montreal.  
327 This indicates that MWO was frequently exposed to northwesterly winds carrying air masses  
328 potentially influenced by anthropogenic emissions in Montreal, while such influences were rare  
329 at WFM. Consequently, much lower baseline CO was found at WFM than at MWO.

330 From April 2001 to December 2010, baseline CO decreased significantly at a rate of  $-2.5$   
331  $\text{ppbv yr}^{-1}$  at TF,  $-4.3 \text{ ppbv yr}^{-1}$  at PSP, and  $-2.8 \text{ ppbv yr}^{-1}$  at WFM. Baseline CO decreased at a  
332 rate of  $-2.3 \text{ ppbv yr}^{-1}$  at MWO over April 2001–March 2009 and  $-3.5 \text{ ppbv yr}^{-1}$  at PM over July  
333 2004–October 2010 (Table 2). Unlike all other sites, CS exhibited an increasing trend of  $2.8$   
334  $\text{ppbv yr}^{-1}$  over April 2001–June 2008. Prior to May 2003, the mixing ratio of baseline CO at CS  
335 was similar to that at TF. After May 2003, baseline CO at CS was  $\sim 30 \text{ ppbv}$  higher than that at  
336 TF and PM (Fig. 2a), resulting in the overall increasing trend. The reasons for such unusually  
337 high values at CS are unknown.

338 The U.S. EPA reported a decrease of 52 % in the national average of annual second  
339 highest 8 h mixing ratios of CO from 2001 to 2010 (EPA, 2012), corresponding to a rate of  $-7.8$   
340  $\text{ppbv yr}^{-1}$  (for an decadal average mixing ratio of  $\sim 150 \text{ ppbv}$ ), which was larger than that at any  
341 of our sites. Because EPA's trend was estimated using measurements mainly from urban sites  
342 with higher concentrations and also focused on the high end of the distribution, it is expected to  
343 show larger changes compared to the trend of baseline levels at rural or remote sites from this  
344 study, with influence of direct anthropogenic emissions removed.

345 The total CO column from MOPITT retrievals over the eastern US was found to decrease  
346 at a rate of  $1.4\% \text{ yr}^{-1}$  (or  $-2.1 \text{ ppbv yr}^{-1}$  for a decadal average mixing ratio of  $\sim 150 \text{ ppbv}$ ) from  
347 2000 to 2011 (Worden et al., 2013), which was comparable to that of the baseline CO in this

348 study. These significant decreasing trends of baseline CO and total column CO were probably  
349 associated in large part with anthropogenic CO emissions reductions worldwide (Gratz et al.,  
350 2014). Globally, anthropogenic CO emissions showed a slight decrease of  $\sim 1\%$  from 1990 to  
351 2010 (Granier et al., 2011). In the US and Europe, total anthropogenic CO emissions declined at  
352 a rate of  $-3\% \text{ yr}^{-1}$  from 2000 to 2010, while increasing trends were found in India ( $\sim 1.5\% \text{ yr}^{-1}$ )  
353 and China ( $\sim 3\% \text{ yr}^{-1}$ ) (Granier et al., 2011). A decreasing trend in CO emissions in China since  
354 2005 was suggested by Tohjima et al. (2014) and Zhang et al. (2009).

### 355 **3.1.2 Baseline O<sub>3</sub>**

356 The baseline O<sub>3</sub> concentrations from all sites ranged from 22 ppbv in the fall to 56 ppbv  
357 in spring, consistent with baseline levels in the Eastern US that were quantified using a principal  
358 component analysis and backward air parcel trajectories by Chan and Vet (2010). The time series  
359 of baseline O<sub>3</sub> at all sites showed averaged annual maxima in April and minima in August–  
360 October (Fig. 2c and d). Annual maxima averaged over their respective periods at the seven sites  
361 occurred all in April and were very close in magnitude, ranging from 47 to 51 ppbv. In  
362 comparison, averaged annual minima at the seven sites displayed distinct difference in  
363 magnitude and timing, varying over 28–37 ppbv, occurring in August at CS, September at AI  
364 and PM, and October at TF, PSP, MWO, and WFM. Studies have suggested that monthly surface  
365 O<sub>3</sub> over remote continental areas generally had a spring maximum, attributed to enhanced  
366 stratospheric input and hemispheric wide photochemical production (Monks, 2000; Parrish et al.,  
367 2013). Here, the fact that baseline CO had annual maxima in spring suggested that the springtime  
368 annual maxima of baseline O<sub>3</sub> were possibly associated with photochemical processing of O<sub>3</sub>  
369 precursors including CO and VOCs that had been built up overwinter on a hemispherical scale  
370 (Kopacz et al., 2010; Penkett et al., 1993).

371 A close examination using the Mann–Kendall test suggested no significant trends in  
372 baseline O<sub>3</sub> during the study period at all sites (Table 2). Similar results were found in Mace  
373 head, Ireland, which is located on the western coast of Europe (Derwent et al., 2007). From 1987  
374 to 1997, baseline O<sub>3</sub> at Mace Head had a significant increasing trend of 0.14 ppbv yr<sup>-1</sup> followed  
375 by a small increase over 1997–1999, and stabilized over 2000–2007 (Derwent et al., 2007).

376 IPCC (2001) suggested that the change of long-term trends in baseline O<sub>3</sub> could be driven  
377 by CH<sub>4</sub> oxidation in the presence of NO<sub>x</sub>. In a polluted region, O<sub>3</sub> is produced by photochemical  
378 reactions of nonmethane hydrocarbons (NMHCs) and NO<sub>x</sub> (West et al., 2006). In the global  
379 troposphere, CH<sub>4</sub> is the primary anthropogenic VOC (Fiore et al., 2002) and affects global  
380 background mixing ratios of O<sub>3</sub> due to its long lifetime (8–9 years). Derwent et al. (2007) found  
381 the change of baseline O<sub>3</sub> in Mace Head followed the mixing ratios of baseline CH<sub>4</sub> over 1992–  
382 2007. West et al. (2006) found that reducing global anthropogenic CH<sub>4</sub> emissions by 20%  
383 beginning in 2010 would reduce O<sub>3</sub> mixing ratios globally by ~ 1 ppbv in 2030. Globally, the  
384 growth rate of CH<sub>4</sub> declined from ~ 13 ppbv yr<sup>-1</sup> in the early 1980s to near zero over 1999–2006  
385 (WMO, 2012). Since 2007, atmospheric CH<sub>4</sub> was increasing again with an average rate of ~ 3  
386 ppbv yr<sup>-1</sup> (WMO, 2012). These changes in CH<sub>4</sub> mixing ratios can potentially lead to changes in  
387 baseline O<sub>3</sub> mixing ratios.

388 On the other hand, global NO<sub>x</sub> emissions did not change overall during the study period  
389 (Granier et al., 2011). Granier et al. (2011) reported that annual NO<sub>x</sub> emissions decreased at a  
390 rate of 1.5 Tg yr<sup>-1</sup> in western Europe, 0.7 Tg yr<sup>-1</sup> in central Europe, ~ 5 Tg yr<sup>-1</sup> in the US over  
391 2001–2010, while increased at a rate of ~ 5 Tg yr<sup>-1</sup> in China and ~ 1.5 Tg yr<sup>-1</sup> in India. Xing et  
392 al. (2015) found varying trends in NO<sub>x</sub> mixing ratios over 1990–2010, with 4.1% in China, -1.4%  
393 in the US, and -1.2% in Europe. The annual rates of change in NO<sub>x</sub> concentrations were

394 comparable to those in emissions (Xing et al., 2015). This suggests that increasing CH<sub>4</sub> and  
395 opposite trends of NO<sub>x</sub> emissions worldwide probably contributed to the insignificant trends in  
396 baseline O<sub>3</sub> over the northeast US during 2001–2010.

### 397 **3.2 Seasonal variation of decadal trends in baseline CO and O<sub>3</sub>**

398 Generally a decreasing trend was found in baseline CO and no trend in baseline O<sub>3</sub>  
399 during the decade 2001–2010 as shown in the previous section. However, trends of baseline CO  
400 and O<sub>3</sub> were found to vary by season (Table 2). Baseline CO at CS was anomalously high since  
401 May 2003 (Fig. 2a) and had increased over the decade in all seasons. As the reasons for the  
402 unusually high values at CS are unknown, baseline CO at CS was not included in the subsequent  
403 discussion.

404 In spring and winter, baseline CO at PM, TF, and PSP decreased significantly at a rate  
405 between  $-6.5$  to  $-3.7$  ppbv yr<sup>-1</sup>, while no significant decreasing trends were found at the two  
406 highest sites MWO and WFM (Table 2). In summer, baseline CO at MWO, PM, TF, and PSP  
407 showed decreasing trends varying between  $-5.5$  and  $-4.3$  ppbv yr<sup>-1</sup>. In fall, baseline CO at all  
408 sites decreased significantly at rates varying between  $-6.4$  and  $-3.2$  ppbv yr<sup>-1</sup>.

409 The overall insignificant change of baseline CO at MWO and WFM in spring and winter  
410 could be due to the combined effect of decreasing US emissions and increasing Asian emissions.  
411 MWO and WFM are the highest sites situated close to the top of the daytime convective  
412 boundary layer, which are more likely impacted by free tropospheric air compared to other sites.  
413 Thus, the impact of continental to intercontinental transport could be just as important there, and  
414 perhaps at times more important, than regional transport. CO emissions in the US declined at a  
415 rate of  $\sim -3$  %yr<sup>-1</sup> over 2000–2010, while an overall increasing trend was seen in China over  
416 1999–2010, despite a small decrease since 2005 (Granier et al., 2011; Tohjima et al., 2014).

417 Liang et al. (2004), using GEOS-Chem model simulations, found that Asian influence was  
418 strongest in spring in the North Pacific lower troposphere, due to the combined effect of efficient  
419 ventilation of the Asian boundary layer via midlatitudinal cyclones and convection, long lifetime  
420 of CO, and strong springtime biomass burning emissions in southeastern Asia. The same study  
421 also found that the Asian influence weakened in summer due to the shorter lifetime of CO and  
422 continental export driven most often by convective injection to the upper troposphere, while  
423 particularly strong transpacific transport events occurred in spring and winter (Liang et al., 2004).

424 In fall, baseline O<sub>3</sub> did not show significant trends at any of the sites (Table 2). In  
425 summer, baseline O<sub>3</sub> showed distinct decreasing trends of -3.1 ppbv yr<sup>-1</sup> at AI, -4.7 ppbv yr<sup>-1</sup> at  
426 both MWO and WFM during their respective time periods, and no trends were found at other  
427 sites (Table 2). TF was the only site where baseline O<sub>3</sub> increased significantly at a rate of 2.4  
428 ppbv yr<sup>-1</sup> in spring and 2.7 ppbv yr<sup>-1</sup> in winter over 2001–2010, while other sites showed no  
429 trends during the two seasons.

430 Tropospheric O<sub>3</sub> has been changing over the past four decades in response to changes in  
431 anthropogenic and natural emissions, stratosphere-tropospheric exchange, pollution transport  
432 pathways and O<sub>3</sub> photochemistry (Parrish et al., 2013). Therefore, it was hypothesized that the  
433 following factors may have contributed to the significant decreasing trends in summertime  
434 baseline O<sub>3</sub> at AI, MWO, WFM and significant increasing trends in springtime and wintertime  
435 baseline O<sub>3</sub> at TF:

- 436 1. Decreasing and increasing stratospheric intrusion in summer and winter – spring,  
437 respectively;
- 438 2. Decreasing and increasing continental to intercontinental transport of anthropogenic  
439 and natural O<sub>3</sub> precursors in summer and winter – spring, respectively;

- 440 3. Decreasing emissions of NO<sub>x</sub> from electric power generation and motor vehicles;  
441 and  
442 4. Changing pollution transport pathways in winter, spring, and summer.

443 Factor #1 was examined using PV data, as one of the physical characteristics of  
444 stratospheric air is high value of PV. Time series of PV at 350 K showed no trend in PV over the  
445 northeast US during the decade (Fig. 3a). There appeared to be distinct annual cycles in PV with  
446 maxima in winter and minima in summer, averaged  $1.81 \times 10^{-8}$  and  $1.05 \times 10^{-8} \text{ m}^2\text{s}^{-1}\text{kg}$ ,  
447 respectively (Fig. 3a). Hence, stratospheric intrusion probably had a larger impact on the surface  
448 in winter-spring than in summer, which was supported by previous studies (James et al., 2003;  
449 Stohl et al., 2003). Such impact would more likely reach higher than lower elevation locations.  
450 No trends in baseline O<sub>3</sub> at the two highest sites MWO and WFM appeared to be consistent with  
451 what the time series of PV suggested. Moreover, TF, near the sea level (18 m a.s.l.), was less  
452 likely influenced by stratospheric intrusion than all other sites. These points were verified using  
453 the stratospheric O<sub>3</sub> during 2001–2010 from Liu et al. (2013), which suggested, on seasonal  
454 average in the area including all our sites, no contribution to the lowest layer (0.5 km) in summer,  
455 or no significant trends in such contribution in winter-spring. Therefore, it seemed unlikely that  
456 stratospheric intrusion contributed to the springtime and wintertime increasing trends in baseline  
457 O<sub>3</sub> at TF.

458 Significant increases have been reported by Cooper et al. (2012) in springtime and  
459 wintertime free tropospheric O<sub>3</sub> over North America, particularly in air masses originating from  
460 East Asia. The western US with elevated terrain was much more likely to be influenced by  
461 descending free tropospheric air than the eastern US (Cooper et al., 2012). Even if air masses  
462 rich in O<sub>3</sub> originating from East Asia reached the US East Coast, they would most likely have a

463 stronger impact on elevated sites. The fact of no trends at any of the elevated sites in spring or  
464 winter suggested that long-range transport of O<sub>3</sub> and its precursors from Asia was probably not a  
465 cause of increasing springtime and wintertime baseline O<sub>3</sub> at TF (Factor #2).

466 In summer, continental export from East Asia is weaker (Wild and Akimoto, 2001) and  
467 Asian emissions have less impact on US surface O<sub>3</sub> relative to domestic emissions than in winter  
468 and spring (Reidmiller et al., 2009), which ruled out the effect of long-range transport of Asian  
469 emissions on summertime trends in baseline O<sub>3</sub> at our sites. Summer sees the peak of forest fires  
470 (Wotawa et al., 2001). Therefore, changes in emissions of CO and other O<sub>3</sub> precursors from  
471 biomass burning could influence the trends in summertime baseline O<sub>3</sub> and CO (Sect. 3.3.1).

472 Further analysis suggested that decreasing urban emissions of NO<sub>x</sub> quite likely  
473 contributed to the rise in springtime and wintertime baseline O<sub>3</sub> at TF (Factor #3). Tropospheric  
474 NO<sub>2</sub> column over the US declined by 41% in spring and 33% in summer during the period of  
475 1996–2011 (Cooper et al., 2012). Emissions of NO<sub>x</sub> in the US were reduced by 48% over 1990–  
476 2010, largely due to control of emissions from power plants and mobile sources (Xing et al.,  
477 2013). The Northeast US Urban Corridor, extending from Washington D.C. in the south to  
478 Boston in the north, was dominated by mobile combustion emissions of NO<sub>x</sub>. Annual mixing  
479 ratios of NO<sub>2</sub> in New York City decreased at a rate of  $-0.3 \text{ ppbv yr}^{-1}$  over 1980–2007 (Buckley  
480 and Mitchell, 2011). In winter and early spring with weakened photochemical production,  
481 decreased NO<sub>x</sub> emissions in urban areas could cause less loss of O<sub>3</sub> via titration by NO (Liu et al.,  
482 1987; Jacob et al., 1995; Frost et al., 2006; Jonson et al., 2006), and the result could be enhanced  
483 O<sub>3</sub> mixing ratios in urban plumes (Cooper et al., 2010; Wilson et al., 2012). From measurements  
484 at our sites, data points of O<sub>3</sub> were selected corresponding to wind from the urban corridor. It  
485 was found that the 10th percentile mixing ratio of O<sub>3</sub> at TF in air masses from the urban corridor



486 had been increasing at a rate of  $1.81 \text{ ppbv yr}^{-1}$  ( $p = 0.05$ ) in spring and  $1.52 \text{ ppbv yr}^{-1}$  ( $p < 0.01$ )  
487 in winter (Fig. 3b and c). This strongly suggests that decreased  $\text{NO}_x$  emissions in the urban  
488 corridor likely had a significant impact on springtime and wintertime baseline  $\text{O}_3$  at TF whereas  
489 had no similar effects at other sites. In summer with strong photochemistry, decreased emissions  
490 of  $\text{O}_3$  precursors could lead to reductions in peak summertime  $\text{O}_3$  concentrations at surface  
491 continental sites (Cooper et al., 2012; Parrish et al., 2013). No significant change was found in  
492 summertime 10th percentile mixing ratios of  $\text{O}_3$  in air masses from the urban corridor at TF,  
493 which was consistent with the relatively constant summertime baseline  $\text{O}_3$  at TF as  
494 aforementioned.

495         The implementation of the Acid Rain Program and the  $\text{NO}_x$  Budget Trading Program  
496 (NBP) also reduced  $\text{NO}_x$  emissions from the power plants (Xing et al., 2013). In the Ohio River  
497 Valley, where power plants dominate, both  $\text{NO}_2$  column and  $\text{NO}_x$  emissions decreased by 38 and  
498 34% over 1999–2005 (Kim et al., 2006). However, the 10th percentile mixing ratio of  $\text{O}_3$  in air  
499 masses from the southwest did not show any significant change in winter, spring, and summer at  
500 PSP, which is located to the northeast of the Ohio River Valley (Fig. 3b–d).

501         There is interannual variability in transport pathways, temperature, water vapor, solar  
502 radiation, and natural emissions (e.g., lightning, forest fires, and vegetation). A close  
503 examination of the NOAA CRN data revealed that springtime solar radiation at TF was  
504 increasing at a rate of  $24.5 \text{ W m}^{-2} \text{ yr}^{-1}$  ( $p = 0.03$ ) over 2002–2010, with the lowest value of 432  
505  $\text{Wm}^{-2}$  in 2002 (Fig. 3a), while no significant trend was found in winter. Without the value in  
506 spring 2002, the solar radiation flux at TF increased at a rate of  $9.4 \text{ W m}^{-2} \text{ yr}^{-1}$  in spring ( $p =$   
507  $0.02$ ). This trend in springtime solar radiation at TF was possibly related to cloudiness in  
508 response to changing cyclone activity associated with varying atmospheric circulation, which

509 could have affected baseline O<sub>3</sub>. More frequent cyclone activities, wetter conditions associated  
510 with the North Atlantic storm track parallel to the eastern US coast could be possible factors  
511 leading to the very low solar radiation flux in spring 2002. Further research is warranted to fully  
512 understand what may have caused this phenomenon. The impact of changes in weather  
513 conditions and large scale circulation on baseline O<sub>3</sub> was further explored in the following  
514 section.

### 515 **3.3 Factors controlling baseline CO and O<sub>3</sub> in spring and summer**

516 This section further identifies factors impacting the variation of baseline CO and O<sub>3</sub>.  
517 Emphasis was placed on spring and summer, when there are strong intercontinental transport and  
518 photochemistry involving O<sub>3</sub> and CO (Cooper et al., 2010; Emmons et al., 2003), as well as  
519 exceedances of NAAQS.

#### 520 **3.3.1 Impact of wildfires in summer**

521 Large interannual variability in global CO mixing ratios was attributed to variations in  
522 biomass burning emissions (Novelli et al., 2003; Wotawa et al., 2001). Studies (Hecobian et al.,  
523 2011; Oltmans et al., 2010) suggested that biomass burning effluents from Russia and Canada  
524 flowed into North America. In addition, California and Alaska were two US states with  
525 considerable fire emissions of CO, which reportedly impacted the air quality over North America  
526 (McKendry et al., 2011; Real et al., 2007).

527 Fire emissions of CO in summer were estimated using the GFED dataset and MOPITT  
528 retrievals (Fig. 4a and b). The GFED data suggested that massive wildfires occurred in Russia in  
529 2002, 2003, and 2008 with annual CO emissions of 42.1, 71.1, and 35.8 Tg, respectively. Annual  
530 fire emissions from Canada were 17.4 Tg in 2004 and 18.3 Tg in 2010. In Alaska, the largest  
531 fires occurred in 2004 with 13.1 Tg CO emitted, while in California the largest fire emissions of

532 CO were 1.3 Tg in 2008. From 2001 to 2010, the total CO emissions from wildfires in Russia,  
533 Canada, Alaska and California varied from 19.9 to 84.3 Tg, with the lowest and the highest in  
534 2007 and 2003, respectively.

535 To quantify contributions of wildfires from these four areas to summertime baseline CO  
536 levels at our sites, a linear regression model was used together with MOPITT total CO column  
537 retrievals. Monthly CO columns were first correlated with monthly GFED fire emissions of CO  
538 for the four areas. The correlation coefficients were 0.89, 0.81, 0.81, and 0.84 ( $p < 0.01$  for the  
539 four values) for Russia, Canada, California, and Alaska, respectively, suggesting that the  
540 variability in total column CO over those areas was dominated by that of fire emissions.

541 Further, it was found that the contributions of fire emissions from Russia and Canada to  
542 the variability of summertime baseline CO at the 56 sites were averaged to be 37% and 22%,  
543 respectively (Table 3), and their combined contribution was averaged to be 41%. Contributions  
544 from Alaska and California were negligible at these six sites. Globally, there is approximately 1  
545 billion ha closed forest in the boreal region, about two thirds of which is situated in Russia  
546 (Harden et al., 2000). CO emissions from wildfires in Russia and Canada contributed 49.5 and  
547 29.6%, respectively, to the total CO emissions from wildfires in Northern Hemispheric  
548 midlatitudes (30–90°N). Understandably, baseline CO was well correlated to wildfires in Russia  
549 and Canada at most sites except at PSP.

550 The insignificant correlation between baseline CO at PSP and wildfires emissions from  
551 Russia and Canada was possibly due to less dynamical circulation at the site. PSP had the lowest  
552 wind speed of  $0.47 \text{ m s}^{-1}$  amongst all sites based on surface wind speed averaged over summers  
553 of 2001–2010 (Fig. 5a). This appeared to be consistent with the position of PSP relative to the  
554 pressure systems throughout the year (Fig. 5b–e). The climatological seasonal maps of sea level

555 pressure suggest that PSP is located either on the periphery of the subtropical high in summer –  
556 fall, or the periphery of the North American trough, where wind tends to be the weakest. In  
557 comparison, other sites are either located at the top of the boundary layer, and/or tend to be  
558 positioned within the North American trough, more directly under the influence of the westerly  
559 wind often facilitating global transport.

560 Since wildfires provide a substantial source of  $\text{NO}_x$  and hydrocarbons,  $\text{O}_3$  is expected to  
561 form in fire plumes. Some of these air pollutants live long enough to travel over long distances,  
562 which could elevate baseline  $\text{O}_3$  globally (Jaffe et al., 2004). Corresponding to the largest fire  
563 emissions in summer 2003 in Russia (Fig. 4a), baseline CO in that season at all sites reached the  
564 decadal maxima, and baseline  $\text{O}_3$  was the highest of all summers at AI, CS, MWO, TF, and  
565 WFM (Fig. 4c and d). Jaffe et al. (2004) also suggested that emissions from Siberia forest fires in  
566 summer 2003 were transported to North America resulting in enhancements of 23–37 and 5–9  
567 ppbv in summertime baseline CO and  $\text{O}_3$ , respectively, at 10 sites in Alaska, Canada, and the  
568 Pacific Northwest.

569 The second largest summertime baseline CO mixing ratio of the decade was found in  
570 summer 2004 at ~~CS~~, TF, and WFM (Fig. 4c), although the total CO emissions from wildfires in  
571 Russia and Canada during that season was 20.4 Tg, 16% smaller than 24.4 Tg, the decadal  
572 (2001–2010) average annual CO emissions from the two countries. Over Alaska, the  
573 geopotential height in summer 2004 was  $\sim 40$  gpm higher than normal years (Fig. 6a–c). This  
574 relatively higher pressure field led to drier and warmer conditions over Alaska and southwestern  
575 Canada with 82% relative humidity and  $12^\circ\text{C}$  surface temperature, the driest and warmest of the  
576 decade (Fig. 6d). Such weather conditions are conducive to occurrence of wildfires. In summer  
577 2004, CO emissions from wildfires in Canada and Alaska contributed 48.5 and 36.5%,

578 respectively, to the Northern Hemispheric total, compared to the decadal (2001–2010) average  
579 contributions of 49.5, 10.6, and 29.6% from Russia, Alaska, and Canada, respectively.  
580 Correspondingly, the 13.1 Tg CO emissions from wildfires in Alaska were the largest over the  
581 decade, and the 17.4 Tg CO emissions from wildfires in Canada were the second largest of the  
582 decade, following the largest in summer 2010 (Fig. 4a). On the other hand, the streamlines over  
583 Canada suggested an unusually strong northeasterly component in summer 2004. The high  
584 pressure system over Alaska and southwestern Canada most likely strengthened the westward  
585 transport of wildfires effluents from Alaska and Canada (Fig. 6c). The combination of these two  
586 factors resulted in efficient transport of massive CO emissions from fires over Alaska and  
587 Canada. Smoke from these fires over the continental United States was observed in satellite  
588 images of aerosol optical depth (AOD) from the GOES (Geostationary Operational  
589 Environmental Satellites) (Kondragunta et al., 2008) and MODIS (Moderate Resolution Imaging  
590 Spectro-radiometer) aboard Terra (Mathur, 2008), and extensive plumes of enhanced CO  
591 concentrations were captured in MOPITT (Measurements of Pollutants in the Troposphere)  
592 retrievals (Pfister et al., 2005).

593 Mann–Kendall trend analysis indicated no significant decreasing trends in biomass  
594 burning emissions from Alaska, Canada, and California. In contrast, CO emissions from  
595 wildfires in Russia decreased at a rate of  $-0.51 \text{ Tg yr}^{-1}$  ( $p = 0.10$ ). Summertime baseline CO at  
596 MWO, PM, TF, and PSP decreased at a rate between  $-5.5$  and  $-4.3 \text{ ppbv yr}^{-1}$  and baseline  $\text{O}_3$  at  
597 AI, MWO, and WFM decreased at a rate between  $-4.7$  and  $-3.1 \text{ ppbv yr}^{-1}$  (Sect. 3.2). Based on  
598 regression analysis, as a result of a  $0.51 \text{ Tg yr}^{-1}$  decrease in CO emissions from wildfires in  
599 Russia, baseline  $\text{O}_3$  decreased by  $0.04$ – $0.07 \text{ ppbv yr}^{-1}$  ( $p = 0.08$ – $0.10$ ) at AI, MWO, WFM, and  
600 CS, while baseline CO declined by  $0.14$ – $0.22 \text{ ppbv yr}^{-1}$  ( $p = 0.01$ – $0.10$ ) at AI, TF, MWO, and

601 WFM. Hence, the decreasing trend of biomass burning emissions in Russia was likely a major  
602 factor causing the decreasing trends in baseline CO and O<sub>3</sub> in summer at our sites.

### 603 **3.3.2 Impact of cyclone activity and AO in summer**

604 Meteorology is another factor that can influence summertime baseline CO and O<sub>3</sub> across  
605 the northeast US over 2001–2010. Of all the meteorological variables, midlatitude cyclone  
606 frequency is an important one that can impact regional air quality greatly. It affects not only  
607 boundary layer ventilation, humidity, solar radiation, and temperature but also general circulation  
608 of the regional atmosphere (Leibensperger et al., 2008).

609 Time series of summertime counts of cyclones in the northeast US showed strong  
610 interannual variability (Fig. 7a). The counts of cyclones in 2003, 2006, 2008, 2009, and 2010  
611 were greater than 12, the average of summer 2001–2010. Summer 2009 experienced the largest  
612 number of cyclones (20) passing the northeast US during the 2001–2010 period. Other summers  
613 experienced below-average cyclones. No overall trend was found in the counts of cyclones  
614 during the study period. Our calculated numbers of cyclones were consistent with the results for  
615 the same years from Leibensperger et al. (2008) and Bauer and Del Genio (2006).

616 In summer, cyclones tend to move around the 500 hPa vortex, which is over the cold  
617 Arctic Ocean with broadly symmetric flow around it (Serreze et al., 2007). On the North  
618 American side, the high latitude flow on the 500 hPa pressure level has a southward component,  
619 which tends to steer systems away from the Arctic Ocean (Fig. 7b). Composite analyses  
620 associated with years of strong (2003, 2006, 2008, 2009, and 2010) vs. weak (2001, 2002, 2004,  
621 2005, and 2007) cyclone activities revealed distinct differences in regional to large scale  
622 circulation (Fig. 7c). There turned out to be a pronounced positive difference of ~ 35 gpm  
623 centered over Baffin Island (north of the northeast US) and a negative difference of ~ 25 gpm

624 centered over the northeast US (Fig. 7c). This difference was related to the negative phase of AO  
625 (Fig. 7a), when surface pressure is abnormally high in the polar region and low in the  
626 midlatitudes (Archambault et al., 2008). In a negative AO season, Arctic lows and westerlies are  
627 weaker, leading to more frequent cold-air outbreaks down to Eurasia and the US, and stormy  
628 weather over the Mediterranean (Hess and Lamarque, 2007), and ultimately low baseline CO and  
629 O<sub>3</sub> across the northeast US.

630 A case in point was summer 2009 with the largest cyclone count (20) and the strongest  
631 negative AO phase (-0.92) of the decade (Fig. 7a). Consistent with earlier results, the difference  
632 of 500 hPa geopotential height between summer 2009 and the 10 year average had negative  
633 anomalies up to ~ -60 gpm over the North American continent and positive anomalies up to ~  
634 65 gpm centered near the pole (Fig. 7d). The sea level pressure field (Fig. 7e) featured a  
635 pronounced mean low over southern Canada and the streamlines suggested an unusually strong  
636 northeasterly component. Indeed, the frequency distribution of wind direction at each site  
637 suggested more frequent occurrence of northeasterly wind (22.5–112.5°), with 21% at PM, 9% at  
638 MWO, 42% at TF, 11% at PSP, and 13% at WFM (Fig. 8). In summer 2009, the northeast US  
639 was more often under the influence of cold frontal passages associated with the largest number  
640 of cyclones passing through the region. As a result, the northeast US was exposed most  
641 frequently to air masses of Arctic origin. Moreover, emissions from large scale wildfires clearly  
642 had global effects as discussed in Sect. 3.3.1. In summer 2009, ~ 11.9 Tg CO, the lowest of the  
643 decade, was emitted from wildfires in Russia and Canada (Fig. 7f). Hence, the lowest fire  
644 emissions of CO and the most frequent cyclone activities were likely two important factors  
645 leading to the lowest summertime baseline CO and O<sub>3</sub> in 2009 at the study sites.

646 A contrasting case was summer 2003, when AO was negative and 15 cyclones passed the  
647 region (Fig. 7a), 25% greater than the decadal mean (12), and yet baseline CO and O<sub>3</sub> at the sites  
648 reached the decadal maxima (Figs. 4c, d and 7f). According to the analysis above, baseline CO  
649 and baseline O<sub>3</sub> were expected to be lower during this summer than the decadal average as a  
650 result of above-average passages of cyclones. However, in summer 2003 CO emissions from  
651 Russian and Canadian wildfires were the largest of the decade (Sect. 3.3.1), counteracting the  
652 effect of the AO. Another interesting example was summer 2007 which had the lowest cyclone  
653 activity of the decade (Fig. 7a), and the total CO emissions from wildfires in Russia and Canada  
654 were 13.6 Tg, the second lowest of the decade following summer 2009 (Fig. 7f). The site-  
655 average baseline CO and O<sub>3</sub> levels in summer 2007 were below the decadal means. Therefore,  
656 the effect of biomass burning may dominate over that of AO and cyclone activity during some  
657 summers, while the two worked in concert during others.

658 Overall, no distinct correlation between counts of cyclones and baseline O<sub>3</sub> was found at  
659 most sites (AI, CS, MWO, PM, TF, WFM), while no significant correlation between counts of  
660 cyclones and baseline CO was found at any of the sites. The only exception was PSP where the  
661 count of cyclones was found to be reasonably anti-correlated with baseline O<sub>3</sub> ( $r = -0.56$ ,  $p =$   
662  $0.05$ ) in the summer. As discussed in Sect. 3.3.1, PSP was the only site that did not seem to be  
663 affected by the Russian and Canadian wildfire emissions as all other sites were, possibly due to  
664 its being situated in a region less impacted by large-scale dynamics. Perhaps this very dynamic  
665 characteristic cast the site under a predominant influence of synoptic systems, e.g., the Bermuda  
666 High and cold frontal passages. As commonly known, high mixing ratios of O<sub>3</sub> in the northeast  
667 occur under summertime stagnant, clear sky conditions associated with the Bermuda High  
668 (Logan, 1989; Vukovich, 1995; Hegarty et al., 2007; Lai et al., 2012), while low O<sub>3</sub> was often



669 linked to cold fronts which sweep out polluted air leaving much cooler and cleaner air in the  
670 northeast (Cooper et al., 2001; Leibensperger et al., 2008; Li et al., 2005). Conceivably, with  
671 more frequent cyclones passing the northeast US, lower concentrations of baseline CO and O<sub>3</sub>  
672 would be expected, and the predominant effect of such synoptic systems could quite likely lead  
673 to anticorrelation between the baseline CO/O<sub>3</sub> levels and cyclone activities.

### 674 3.3.3 Impact of NAO in spring (March and April)

675 Wildfires in March and April were scarce, with mean CO emissions of 1.78 Tg in Russia  
676 and 0.004 Tg in Canada over 2001–2010, negligible compared to emissions during the fire  
677 season (May–September). To focus on the impact of large circulation patterns on baseline CO  
678 and O<sub>3</sub> in spring, the May data were excluded to avoid the effect of biomass burning. Springtime  
679 baseline O<sub>3</sub> at each site showed strong and consistent interannual variation up to 10 ppbv (Fig.  
680 9a). The baseline O<sub>3</sub> mixing ratio averaged at all the seven sites over the decade was 46.5 ppbv,  
681 and exceeded the average (>46.5 ppbv) in 2001, 2003, 2005, 2008, 2010, and was below average  
682 ( $\leq 46.5$  ppbv) in 2002, 2004, 2006, 2007, 2009 (Fig. 9a).

683 The difference of 850 hPa geopotential height between the lower and higher O<sub>3</sub> years is  
684 shown in Fig. 10. There was a pronounced difference up to 40 gpm in the Bermuda/Azores high  
685 and  $\sim -40$  gpm in the Icelandic low, which resulted in stronger gradient flow between the two  
686 pressure systems ~~and was indicative of the positive phase of NAO, known as the positive phase~~  
687 ~~of NAO~~. Over 2001–2010, NAO index was significantly positive in 2002, 2004, 2007, 2009 and  
688 negative in 2001, 2005, 2008, 2010, which corresponded mostly to the years of below and above  
689 the decadal average baseline O<sub>3</sub>, respectively. Significant negative correlation was found between  
690 the NAO index and baseline O<sub>3</sub> at each site (Table 4) (~~CS:  $r = -0.75$ ,  $p = 0.03$ ; MWO:  $r = -0.68$ ,~~  
691  ~~$p = 0.03$ ; PM:  $r = -0.81$ ,  $p = 0.03$ ; TF:  $r = -0.81$ ,  $p < 0.01$ ; PSP:  $r = -0.58$ ,  $p = 0.06$ ; WFM:  $r =$~~

692 |  ~~$-0.51, p = 0.10$~~ . The negative correlation between baseline O<sub>3</sub> and the NAO index could be a  
693 | result of multiple factors, such as solar flux, stratosphere-tropospheric exchange, and continental  
694 | export of O<sub>3</sub> produced in North America. ~~It should be noted that, no significant correlation was~~  
695 | ~~found between the NAO index and baseline CO at any of the sites, which suggests that NAO is~~  
696 | ~~not linked to or played an insignificant role in the interannual variability of baseline CO.~~

697 | The first possible explanation for the baseline O<sub>3</sub> and NAO index anticorrelation was  
698 | changes in surface solar radiation flux during positive/negative NAO years. During a positive  
699 | NAO year, the mean North Atlantic storm track parallels the eastern North American coastline  
700 | before extending northeastward to near Iceland (Rogers, 1997). This storm track and its  
701 | associated moisture transport and convergence lead to relatively wet conditions near the eastern  
702 | US coast (Archambault et al., 2008; Hurrell, 1995). During a negative NAO year, the mean  
703 | North Atlantic storm track is more zonal (Rogers, 1997), leading to relatively dry conditions near  
704 | the eastern US coast (Archambault et al., 2008; Hurrell, 1995). At ~~our coastal~~ sites around the  
705 | northeast US coast (CS and TF), significant correlation was found between relative humidity and  
706 | the NAO index (~~CS:  $r = 0.85, p = 0.02$ ; TF:  $r = 0.64, p = 0.06$~~ ), while the correlation was weaker  
707 | at inland, elevated sites (PSP and WFM) (~~PSP:  $r = 0.23, p = 0.26$ ; WFM:  $r = 0.40, p = 0.13$~~ )  
708 | (Table 4 and Fig. 9b).

709 | During positive NAO years, wetter conditions indicate higher relative humidity and more  
710 | cloudiness, most likely leading to reduced solar radiation flux near the surface and subsequently  
711 | less O<sub>3</sub> production. As expected, a significant negative correlation was found between relative  
712 | humidity and solar radiation ( ~~$r = -0.67, p = 0.05$~~ ) (~~Fig. 9b~~) and a significant positive correlation  
713 | between baseline O<sub>3</sub> and solar radiation flux ( ~~$r = 0.75, p = 0.03$~~ ) at TF in March and April (Table  
714 | 4 and Fig. 9b). No significant correlation between these variables was found in other seasons.

715 Another possible explanation for the negative correlation between NAO index and  
716 baseline O<sub>3</sub> was the influence of stratospheric intrusion. Dynamically, the North American  
717 trough induces descending air on its tailing side and in the upper troposphere it can cause  
718 tropopause folding with stratospheric air mixing downward into the troposphere. The difference  
719 of the PV patterns between positive NAO years and negative NAO years is illustrated in Fig. 11.  
720 Negative anomalies of  $\sim -0.6 \times 10^{-9} \text{ m}^2 \text{ s}^{-1} \text{ kg}$  were found over the northeast US, suggesting that  
721 positive NAO was related to less stratospheric intrusion (Hess and Lamarque, 2007) over the  
722 northeast US. This is consistent with lower baseline O<sub>3</sub> levels during positive NAO springs. This  
723 was further verified using the stratospheric O<sub>3</sub> dataset constructed by Liu et al. (2013).  
724 Stratospheric O<sub>3</sub> was hardly detected at the lowest two layers (i.e., 0.5 and 1.5 km) in April. In  
725 March,  $\sim 40\text{--}60$  ppbv of stratospheric O<sub>3</sub> reached the lowest layer in our study area in 2004 and  
726 2006–2008 and reached the 1.5 km layer in 2001–2008. The stratospheric contribution to the 0.5  
727 km layer was the largest in March 2008, when NAO was negative (Fig. 9).

728 The third possible factor affecting baseline O<sub>3</sub> over the northeast US was the effect of  
729 North American continental export. During a positive NAO phase, the anticyclonic circulation  
730 off the US east coast and the cyclonic circulation across the North Atlantic were amplified with a  
731 northward shift (Rogers, 1997). As a result, stronger surface wind was found near 50°N across  
732 the North Atlantic basin and into Northern Europe (Hess and Lamarque, 2007). Annual wind  
733 speed from the west (247.5–337.5°) was calculated at the study sites (Fig. 9c). Positive  
734 correlation was found between surface wind and NAO index at [MWO, CS, and TF \(Table 4\)](#)  
735 [most sites \(MWO:  \$r = 0.76, p = 0.02\$ ; CS:  \$r = 0.68, p = 0.06\$ ; TF:  \$r = 0.57, p = 0.09\$ \)](#). Eckhardt et  
736 al. (2004) found that the warm conveyor belt over the northeast US coast occurred  $\sim 12\%$  more  
737 frequently in positive NAO years than in negative NAO years. The ending trajectories of the

738 warm conveyor belt in positive NAO years extended further eastward into western and northern  
739 Europe (Eckhardt et al., 2004). It was suggested that in a positive NAO year, the O<sub>3</sub> produced  
740 over the northeast US was less likely accumulated in the region, and was more likely transported  
741 faster off the continent and across the Atlantic Ocean. These changes were consistent with the  
742 positive anomalies of O<sub>3</sub> observed over northwestern Europe (Christoudias et al., 2012; Eckhardt  
743 et al., 2003). Negative correlation, although insignificant, was also found between baseline CO  
744 and the NAO index at most of our study sites (Table 4). North American continental export  
745 could also impact the variation of baseline CO, while this impact could be confounded by other  
746 factors, e.g. stratospheric intrusion. Specifically, during positive NAO years, more continental  
747 outflows lead to a decrease in baseline CO, while less stratospheric intrusion would lead to less  
748 dilution of surface CO and thus increase baseline CO levels. Further research is warranted to  
749 fully understand the relationship between baseline CO and NAO.

#### 750 **4 Summary**

751 Baseline CO and O<sub>3</sub> at seven rural sites in the northeast US were examined for their  
752 seasonal and interannual variabilities during the time period of 2001–2010, and potential  
753 mechanisms controlling the variabilities were investigated. It was found that baseline CO at most  
754 sites (MWO, PM, TF, PSP, and WFM) decreased significantly at a rate between –4.3 to –2.3  
755 ppbv yr<sup>-1</sup>, while baseline O<sub>3</sub> was relatively constant. No trends were found in baseline O<sub>3</sub> at all  
756 sites probably resulting from relatively constant mixing ratios of CH<sub>4</sub> in the 2000s and opposite  
757 rates of change in NO<sub>x</sub> emissions around the world.

758 In spring and winter, baseline CO at MWO and WFM did not exhibit a significant trend,  
759 possibly a result of the combined effect of decreasing emissions in the northeast US and  
760 increasing emissions in Asia. TF, a coastal rural site, was the only location where baseline O<sub>3</sub>

761 was found to increase significantly at a rate of 2.4 and 2.7 ppbv yr<sup>-1</sup> in spring and winter,  
762 respectively, most likely caused by the decrease in NO<sub>x</sub> emissions over the urban corridor.

763 It was found that interannual variations of baseline CO and O<sub>3</sub> were predominantly  
764 influenced by biomass burning emissions, cyclone activities, and NAO. In summer, ~ 38% of  
765 baseline CO variability was attributed to CO emissions from forest fires in Russia and ~ 22% to  
766 emissions from forest fires in Canada. The lowest mixing ratios of baseline CO and O<sub>3</sub> at most  
767 sites in summer 2009 were linked to frequent cyclone activity, which were induced by the  
768 unusually weak low pressure system in the Arctic region. In spring, a significant negative  
769 correlation was found between baseline O<sub>3</sub> and the NAO index, potentially due to variations of  
770 solar flux, stratospheric intrusion, and continental export.

771 On 1 October 2015 the U.S. EPA lowered the NAAQS for ground-level O<sub>3</sub> to 70 ppbv ~~In~~  
772 ~~December 2014, the U.S. EPA proposed to tighten the 2008 NAAQS for daily maximum 8 h~~  
773 ~~average O<sub>3</sub> from 75 ppbv to a level within a range of 65–70 ppbv to provide to improve~~  
774 protection of public health and welfare (EPA, 2014) ([http://www3.epa.gov/ozonepollution/pdfs/](http://www3.epa.gov/ozonepollution/pdfs/20151001overviewfs.pdf)  
775 [20151001overviewfs.pdf](http://www3.epa.gov/ozonepollution/pdfs/20151001overviewfs.pdf)). As the O<sub>3</sub> NAAQS are set closer to background levels, states will face  
776 ever increasing challenges with regard to fulfilling their obligation for NAAQS attainment.  
777 Through this study it was reinforced that, in addition to domestic emission control,  
778 intercontinental transport of anthropogenic emissions and wildfires emissions together with  
779 meteorological conditions should be considered for an encompassing, cost-effective emission  
780 control strategy that accounts for impacts of regional to global emissions and moreover  
781 emissions of multi-pollutants (e.g., CO, CH<sub>4</sub>, NO<sub>x</sub>, and NMHCs). In addition, the relationships  
782 between baseline O<sub>3</sub>/CO and various factors (e.g. NO<sub>x</sub> emission controls, biomass burning  
783 emissions, NAO, and AO) examined in this study can also be used as reference point for

784 evaluating global/regional air quality modeling systems that are used in air quality management  
785 applications. One limitation of this study is that it was based on ten-year observations, and hence  
786 it was unlikely to predict the potential changes in natural emissions and AO/NAO signals as well  
787 as their impacts on baseline O<sub>3</sub>. Future research is warranted to further address the issues  
788 identified in this work on climatological time scales.

789 *Acknowledgements.* This work was funded by the Environment Protection Agency grant  
790 #83521501. We are grateful to Z. Ye, Y. Zhang, R. D. Yanai, G. Townsend, and E. P. Law for  
791 their valuable suggestions and help. We thank K. Cochrane and K. Yan for their assistance in the  
792 early stage of the study.

793 *Disclaimer.* Although this work has been reviewed and approved for publication by the U.S.  
794 Environmental Protection Agency (EPA), it does not reflect the views and policies of the agency.

795

## 796 **References**

797 Archambault, H. M., Bosart, L. F., Keyser, D., and Aiyyer, A. R.: Influence of large-scale flow  
798 regimes on cool-season precipitation in the northeastern United States, *Mon. Weather Rev.*, 136,  
799 2945–2963, doi:10.1175/2007MWR2308.1, 2008.

800 Bae, M. S., Schwab, J. J., Chen, W. N., Lin, C. Y., Rattigan, O. V., and Demerjian, K. L.:  
801 Identifying pollutant source directions using multiple analysis methods at a rural location in New  
802 York, *Atmos. Environ.*, 45, 2531–2540, doi:10.1016/j.atmosenv.2011.02.020, 2011.

803 Barnston, A. G. and Livezey, R. E.: Classification, seasonality and persistence of low-frequency  
804 atmospheric circulation patterns, *Mon. Weather Rev.*, 115, 1083–1126, 1987.

805 Bauer, M. and Del Genio, A. D.: Composite analysis of winter cyclones in a GCM: influence on  
806 climatological humidity, *J. Climate*, 19, 1652–1672, doi:10.1175/JCLI3690.1, 2006.

807 Bell, M. L., Goldberg, R., Hogrefe, C., Kinney, P. L., Knowlton, K., Lynn, B., Rosenthal, J.,  
808 Rosenzweig, C., and Patz, J. A.: Climate change, ambient ozone, and health in 50 US cities,  
809 *Clim. Change*, 82, 61–76, doi:10.1007/s10584-006-9166-7, 2007.

810 Brand, S., Dethloff, K., and Handorf, D.: Tropospheric circulation sensitivity to an interactive  
811 stratospheric ozone, *Geophys. Res. Lett.*, 35, 1–5, doi:10.1029/2007GL032312, 2008.

812 Brandt, R. E., Schwab, J. J., Casson, P. W., Roychowdhury, U. K., Wolfe, D., Demerjian, K. L.,  
813 Civerolo, K. L., Rattigan, O. V., and Felton, H. D.: Atmospheric chemistry measurements at  
814 Whiteface Mountain, NY: ozone and reactive trace gases, *Aerosol and Air Quality Research*,  
815 submitted to special issue, 2015.

816 Buckley, S. M. and Mitchell, M. J.: Improvements in urban air quality: case studies from New  
817 York state, USA, *Water Air Soil Poll.*, 214, 93–106, doi:10.1007/s11270-010-0407-z, 2011.

818 Chan, E.: Regional ground-level ozone trends in the context of meteorological influences across  
819 Canada and the eastern United States from 1997 to 2006, *J. Geophys. Res.-Atmos.*, 114, 1–18,  
820 doi:10.1029/2008JD010090, 2009.

821 Chan, E. and Vet, R. J.: Baseline levels and trends of ground level ozone in Canada and the  
822 United States, *Atmos. Chem. Phys.*, 10, 8629–8647, doi:10.5194/acp-10-8629-2010, 2010.

823 Christoudias, T., Pozzer, A., and Lelieveld, J.: Influence of the North Atlantic Oscillation on air  
824 pollution transport, *Atmos. Chem. Phys.*, 12, 869–877, doi:10.5194/acp-12-869-2012, 2012.

825 Cooper, O. R., Moody, J. L., Parrish, D. D., Trainer, M., Ryerson, T. B., Holloway, J. S., Hübler,  
826 G., Fehsenfeld, F. C., Oltmans, S. J., and Evans, M. J.: Trace gas signatures of the airstreams  
827 within North Atlantic cyclones: case studies from the North Atlantic Regional Experiment  
828 (NARE '97) aircraft intensive, *J. Geophys. Res.-Atmos.*, 106, 5437–5456,  
829 doi:10.1029/2000JD900574, 2001.

830 Cooper, O. R., Parrish, D. D., Stohl, A., Trainer, M., Nédélec, P., Thouret, V., Cammas, J. P.,  
831 Oltmans, S. J., Johnson, B. J., Tarasick, D., Leblanc, T., McDermid, I. S., Jaffe, D., Gao, R.,  
832 Stith, J., Ryerson, T., Aikin, K., Campos, T., Weinheimer, A., and Avery, M. A.: Increasing  
833 springtime ozone mixing ratios in the free troposphere over western North America, *Nature*, 463,  
834 344–348, doi:10.1038/nature08708, 2010.

835 Cooper, O. R., Gao, R. S., Tarasick, D., Leblanc, T., and Sweeney, C.: Long-term ozone trends  
836 at rural ozone monitoring sites across the United States, 1990–2010, *J. Geophys. Res.-Atmos.*,  
837 117, 1990–2010, doi:10.1029/2012JD018261, 2012.

838 Creilson, J. K., Fishman, J., and Wozniak, A. E.: Intercontinental transport of tropospheric ozone:  
839 a study of its seasonal variability across the North Atlantic utilizing tropospheric ozone residuals  
840 and its relationship to the North Atlantic Oscillation, *Atmos. Chem. Phys.*, 3, 2053–2066,  
841 doi:10.5194/acp-3-2053-2003, 2003.

842 Creilson, J. K., Fishman, J., and Wozniak, A. E.: Arctic oscillation-induced variability in  
843 satellitederived tropospheric ozone, *Geophys. Res. Lett.*, 32, 1–5,  
844 doi:10.1029/2005GL023016, 2005.

845 Cui, J., Pandey Deolal, S., Sprenger, M., Henne, S., Staehelin, J., Steinbacher, M., and Nédélec,  
846 P.: Free tropospheric ozone changes over Europe as observed at Jungfraujoch (1990–2008): an  
847 analysis based on backward trajectories, *J. Geophys. Res.-Atmos.*, 116, 1–14,  
848 doi:10.1029/2010JD015154, 2011.

849 Daniel, J. S. and Solomon, S.: On the climate forcing of carbon monoxide, *J. Geophys. Res.*  
850 *Atmos.*, 103, 13249–13260, doi:10.1029/98JD00822, 1998.



851 Derwent, R. G., Simmonds, P. G., Manning, A. J., and Spain, T. G.: Trends over a 20-year  
852 period from 1987 to 2007 in surface ozone at the atmospheric research station, Mace Head,  
853 Ireland, *Atmos. Environ.*, 41, 9091–9098, doi:10.1016/j.atmosenv.2007.08.008, 2007.

854 Duncan, B. N. and Bey, I.: A modeling study of the export pathways of pollution from Europe:  
855 seasonal and interannual variations (1987–1997), *J. Geophys. Res.-Atmos.*, 109, D08301,  
856 doi:10.1029/2003JD004079, 2004.

857 Dutkiewicz, V. A., Husain, L., Roychowdhury, U. K., and Demerjian, K. L.: Impact of Canadian  
858 wildfire smoke on air quality at two rural sites in NY state, *Atmos. Environ.*, 45, 2028–  
859 2033, doi:10.1016/j.atmosenv.2011.01.072, 2011.

860 Eckhardt, S., Stohl, A., Beirle, S., Spichtinger, N., James, P., Forster, C., Junker, C., Wagner, T.,  
861 Platt, U., and Jennings, S. G.: The North Atlantic Oscillation controls air pollution transport to  
862 the Arctic, *Atmos. Chem. Phys.*, 3, 1769–1778, doi:10.5194/acp-3-1769-2003, 2003.

863 Eckhardt, S., Stohl, A., Wernli, H., James, P., Forster, C., and Spichtinger, N.: A 15-year  
864 climatology of warm conveyor belts, *J. Climate*, 17, 218–237, 2004.

865 Emmons, L. K., Hess, P., Klonecki, A., Tie, X., Horowitz, L., Lamarque, J.-F., Kinnison, D.,  
866 Brasseur, G., Atlas, E., Browell, E., Cantrell, C., Eisele, F., Mauldin, R. L., Merrill, J., Ridley, B.,  
867 and Shetter, R.: Budget of tropospheric ozone during TOPSE from two chemical transport  
868 models, *J. Geophys. Res.-Atmos.*, 108, 8372, doi:10.1029/2002JD002665, 2003.

869 Fiore, A. M., Jacob, D. J., Bey, I., Yantosca, R. M., Field, B. D., Fusco, A. C., and Wilkinson, J.  
870 G.: Background ozone over the United States in summer: origin, trend, and contribution to  
871 pollution episodes, *J. Geophys. Res.-Atmos.*, 107, ACH 11-1–ACH 11-25,  
872 doi:10.1029/2001JD000982, 2002.

873 Frost, G. J., McKeen, S. A., Trainer, M., Ryerson, T. B., Neuman, J. A., Roberts, J. M., Swanson,  
874 A., Holloway, J. S., Sueper, D. T., Fortin, T., Parrish, D. D., Fehsenfeld, F. C., Flocke, F.,  
875 Peckham, S. E., Grell, G. A., Kowal, D., Cartwright, J., Auerbach, N., and Habermann,  
876 T.: Effects of changing power plant NO<sub>x</sub> emissions on ozone in the eastern United States: proof  
877 of concept, *J. Geophys. Res.-Atmos.*, 111, D12306, doi:10.1029/2005JD006354, 2006.

878 Granier, C., Bessagnet, B., Bond, T., D'Angiola, A., van der Gon, H. D., Frost, G. J., Heil, A.,  
879 Kaiser, J. W., Kinne, S., Klimont, Z., Kloster, S., Lamarque, J. F., Liousse, C., Masui, T., Meleux,  
880 F., Mieville, A., Ohara, T., Raut, J. C., Riahi, K., Schultz, M. G., Smith, S. J., Thompson, A., van  
881 Aardenne, J., van der Werf, G. R., and van Vuuren, D. P.: Evolution of anthropogenic and  
882 biomass burning emissions of air pollutants at global and regional scales during the 1980–2010  
883 period, *Clim. Change*, 109, 163–190, doi:10.1007/s10584-011-0154-1, 2011.

884 Gratz, L. E., Jaffe, D. A., and Hee, J. R.: Causes of increasing ozone and decreasing carbon  
885 monoxide in springtime at the Mt. Bachelor Observatory from 2004 to 2013, *Atmos. Environ.*,  
886 109, 323–330, doi:10.1016/j.atmosenv.2014.05.076, 2014.

887 Harden, J. W., Trumbore, S. E., Stocks, B. J., Hirsch, A., Gower, S. T., O'Neill, K. P., and  
888 Kasischke, E. S.: The role of fire in the boreal carbon budget, *Glob. Change Biol.*, 6  
889 (Supplement1), 174–184, doi:10.1046/j.1365-2486.2000.06019.x, 2000.

890 Hecobian, A., Liu, Z., Hennigan, C. J., Huey, L. G., Jimenez, J. L., Cubison, M. J., Vay, S.,  
891 Diskin, G. S., Sachse, G. W., Wisthaler, A., Mikoviny, T., Weinheimer, A. J., Liao, J., Knapp, D.  
892 J., Wennberg, P. O., Kürten, A., Crouse, J. D., Clair, J. St., Wang, Y., and Weber, R. J.:  
893 Comparison of chemical characteristics of 495 biomass burning plumes intercepted by the  
894 NASA DC-8 aircraft during the ARCTAS/CARB-2008 field campaign, *Atmos. Chem. Phys.*, 11,  
895 13325–13337, doi:10.5194/acp-11-13325-2011, 2011.

896 Hegarty, J., Mao, H., and Talbot, R.: Synoptic controls on summertime surface ozone in the  
897 northeastern United States, *J. Geophys. Res.-Atmos.*, 112, D14306, doi:10.1029/2006JD008170,  
898 2007.

899 Hegarty, J., Mao, H., and Talbot, R.: Synoptic influences on springtime tropospheric O<sub>3</sub> and CO  
900 over the North American export region observed by TES, *Atmos. Chem. Phys.*, 9, 3755–3776,  
901 doi:10.5194/acp-9-3755-2009, 2009.

902 Herron-Thorpe, F. L., Mount, G. H., Emmons, L. K., Lamb, B. K., Jaffe, D. A., Wigder, N.  
903 L., Chung, S. H., Zhang, R., Woelfle, M. D., and Vaughan, J. K.: Air quality simulations of  
904 wildfires in the Pacific Northwest evaluated with surface and satellite observations during the  
905 summers of 2007 and 2008, *Atmos. Chem. Phys.*, 14, 12533–12551, doi:10.5194/acp-14-12533-  
906 2014, 2014.

907 Hess, P. G. and Lamarque, J. F.: Ozone source attribution and its modulation by the Arctic  
908 oscillation during the spring months, *J. Geophys. Res.-Atmos.*, 112, 1–  
909 17, doi:10.1029/2006JD007557, 2007.

910 Honrath, R. E., Owen, R. C., Val Martín, M., Reid, J. S., Lapina, K., Fialho, P., Dziobak, M. P.,  
911 Kleissl, J., and Westphal, D. L.: Regional and hemispheric impacts of anthropogenic and  
912 biomass burning emissions on summertime CO and O<sub>3</sub> in the North Atlantic lower free  
913 troposphere, *J. Geophys. Res.-Atmos.*, 109, 1–17, doi:10.1029/2004JD005147, 2004.

914 Task Force on Hemispheric Transport of Air Pollution (TF HTAP): Hemispheric transport of air  
915 pollution 2010 assessment report, edited by: Keating, T. J. and Zuber, A., draft, available at:  
916 <http://www.htap.org>, 2010.

917 Hu, Q., Tawaye, Y., and Feng, S.: Variations of the Northern Hemisphere atmospheric energetics:  
918 1948–2000, *J. Climate*, 17, 1975–1986, doi:10.1175/1520-  
919 0442(2004)017<1975:VOTNHA>2.0.CO;2, 2004.

920 Hurrell, J. W.: Decadal trends in the north atlantic oscillation: regional temperatures and  
921 precipitation, *Science*, 269, 676–679, doi:10.1126/science.269.5224.676, 1995.

922 Intergovernmental Panel on Climate Change (IPCC): Climate Change 2001: The Scientific Basis,  
923 *Clim. Change 2001 Sci. Basis*, 881, doi:10.1256/004316502320517344, 2001.

924 Intergovernmental Panel on Climate Change (IPCC), Climate Change 2007: The Physical  
925 Science Basis, in: Contribution of Working Group I to the Fourth Assessment Report of the  
926 Intergovernmental Panel on Climate Change, edited by: Solomon, S., Qin, D., Manning, M.,  
927 Chen, Z., Marquis, M., Averyt, K. B., Tignor M., and Miller H. L., Cambridge University Press,  
928 Cambridge, UK and New York, NY, USA, 2007.

929 Jacob, D. J.: Seasonal transition from NO<sub>x</sub>- to hydrocarbon-limited conditions for ozone  
930 production over the eastern United States in september, *J. Geophys. Res.*, 100, 9315–9324,  
931 doi:10.1029/94JD03125, 1995.

932 Jaffe, D., Bertsch, I., Jaeglé, L., Novelli, P., Reid, J. S., Tanimoto, H., Vingarzan, R., and  
933 Westphal, D. L.: Long-range transport of Siberian biomass burning emissions and impact on  
934 surface ozone in western North America, *Geophys. Res. Lett.*, 31, 6–9,  
935 doi:10.1029/2004GL020093, 2004.

936 James, P., Stohl, A., Forster, C., Eckhardt, S., Seibert, P., and Frank, A.: A 15-year climatology  
937 of stratosphere–troposphere exchange with a Lagrangian particle dispersion model 2. Mean  
938 climate and seasonal variability, *J. Geophys. Res.-Atmos.*, 108,  
939 8522, doi:10.1029/2002JD002639, 2003.

940 Jonson, J. E., Simpson, D., Fagerli, H., and Solberg, S.: Can we explain the trends in European  
941 ozone levels?, *Atmos. Chem. Phys.*, 6, 51–66, doi:10.5194/acp-6-51-2006, 2006.

942 Kang, C. M., Gold, D., and Koutrakis, P.: Downwind O<sub>3</sub> and PM<sub>2.5</sub> speciation during the  
943 wildfires in 2002 and 2010, *Atmos. Environ.*, 95, 511–519,  
944 doi:10.1016/j.atmosenv.2014.07.008,2014.

945 Kim, S.-W., Heckel, A., McKeen, S. A., Frost, G. J., Hsie, E.-Y., Trainer, M. K., Richter,  
946 A.,Burrows, J. P., Peckham, S. E., and Grell, G. A.: Emission reductions and their impact on air  
947 quality, *Geophys. Res. Lett.*, 33, 1–5, doi:10.1029/2006GL027749, 2006.

948 Kondragunta, S., Lee, P., McQueen, J., Kittaka, C., Prados, A. I., Ciren, P., Laszlo, I.,Pierce, R.  
949 B., Hoff, R., and Szykman, J. J.: Air quality forecast verification using satellitedata, *J. Appl.*  
950 *Meteorol. Clim.*, 47, 425–442, doi:10.1175/2007JAMC1392.1, 2008.

951 Kopacz, M., Jacob, D. J., Fisher, J. A., Logan, J. A., Zhang, L., Megretskaia, I. A., Yantosca, R.  
952 M., Singh, K., Henze, D. K., Burrows, J. P., Buchwitz, M., Khlystova, I., McMillan, W. W.,  
953 Gille, J. C., Edwards, D. P., Eldering, A., Thouret, V., and Nedelec, P.: Global estimates of CO  
954 sources with high resolution by adjoint inversion of multiple satellite datasets(MOPITT, AIRS,  
955 SCIAMACHY, TES), *Atmos. Chem. Phys.*, 10, 855–876, doi:10.5194/acp-10-855-2010, 2010.

956 Krichak, S. O. and Alpert, P.: Signatures of the NAO in the atmospheric circulation during wet  
957 winter months over the Mediterranean region, *Theor. Appl. Climatol.*, 82, 27–  
958 39,doi:10.1007/s00704-004-0119-7, 2005.

959 Kumar, A., Wu, S., Weise, M. F., Honrath, R., Owen, R. C., Helmig, D., Kramer, L., Val Martin,  
960 M., and Li, Q.: Free-troposphere ozone and carbon monoxide over the North Atlantic for 2001–  
961 2011, *Atmos. Chem. Phys.*, 13, 12537–12547, doi:10.5194/acp-13-12537-2013,2013.

962 Lai, T. L., Talbot, R., and Mao, H.: An investigation of two highest ozone episodes during the  
963 last decade in New England, *Atmosphere*, 3, 59–86, doi:10.3390/atmos3010059, 2012.

964 Lamarque, J.-F., and Hess, P. G.: Arctic Oscillation modulation of the Northern Hemisphere  
965 spring tropospheric ozone, *Geophys. Res. Lett.*, 31, L06127, doi:10.1029/2003GL019116,2004.

966 Lefohn, A. S., Shadwick, D., and Oltmans, S. J.: Characterizing changes in surface ozone levels  
967 in metropolitan and rural areas in the United States for 1980–2008 and 1994–2008, *Atmos.*  
968 *Environ.*, 44, 5199–5210, doi:10.1016/j.atmosenv.2010.08.049, 2010.

969 Leibensperger, E. M., Mickley, L. J., and Jacob, D. J.: Sensitivity of US air quality to mid-  
970 latitude cyclone frequency and implications of 1980–2006 climate change, *Atmos. Chem. Phys.*,  
971 8, 7075–7086, doi:10.5194/acp-8-7075-2008, 2008.

972 Liang, Q., Jaeglé, L., Jaffe, D. A., Weiss-Penzias, P., Heckman, A., and Snow, J. A.: Long-range  
973 transport of Asian pollution to the northeast Pacific: seasonal variations and transport pathways  
974 of carbon monoxide, *J. Geophys. Res.-Atmos.*, 109, 1–16, doi:10.1029/2003JD004402, 2004.

975 Li, Q., Jacob, D. J., Bey, I., Palmer, P. I., Duncan, B. N., Field, B. D., Martin, R. V., Fiore, A. M.,  
976 Yantosca, R. M., Parrish, D. D., Simmonds, P. G. and Oltmans, S. J.: Transatlantic transport of  
977 pollution and its effects on surface ozone in Europe and North America, *J. Geophys. Res.-*  
978 *Atmos.*, 107, ACH 4-1–ACH 4-21, doi:10.1029/2001JD001422, 2002.

979 Li, Q., Jacob, D. J., Park, R., Wang, Y., Heald, C. L., Hudman, R., Yantosca, R. M., Martin, R.  
980 V., and Evans, M.: North American pollution outflow and the trapping of convectively lifted  
981 pollution by upper-level anticyclone, *J. Geophys. Res.-Atmos.*, 110, D10301,  
982 doi:10.1029/2004JD005039, 2005.

983 Lin, C.-Y. C., Jacob, D. J., Munger, J. W., and Fiore, A. M.: Increasing background ozone in  
984 surface air over the United States, *Geophys. Res. Lett.*, 27, 3465–3468,  
985 doi:10.1029/2000GL011762, 2000.

986 Liu, J., Tarasick, D. W., Fioletov, V. E., McLinden, C., Zhao, T., Gong, S., Sioris, C., Jin, J. J.,  
987 Liu, G., and Moeini, O.: A global ozone climatology from ozone soundings via trajectory  
988 mapping: a stratospheric perspective, *Atmos. Chem. Phys.*, 13, 11441–11464, doi:10.5194/acp-  
989 13-11441-2013, 2013.

990 Liu, S. C.: Ozone production in the rural troposphere and the implications for regional and global  
991 ozone distributions., *J. Geophys. Res.*, 92, 4191–4207, 1987.

992 Logan, J. A.: Ozone in rural areas of the United States, *J. Geophys. Res.*, 94, 8511–8532, 1989.

993 Logan, J. A., Staehelin, J., Megretskaia, I. A., Cammas, J. P., Thouret, V., Claude, H., DeBacker,  
994 H., Steinbacher, M., Scheel, H. E., Stbi, R., Fröhlich, M., and Derwent, R.: Changes in ozone  
995 over Europe: analysis of ozone measurements from sondes, regular aircraft (MOZAIC) and alpine  
996 surface sites, *J. Geophys. Res.-Atmos.*, 117, 1–23, doi:10.1029/2011JD016952, 2012.

997 Mao, H. and Talbot, R.: Role of meteorological processes in two New England ozone  
998 episodes during summer 2001, *J. Geophys. Res.-Atmos.*, 109, 1–17,  
999 doi:10.1029/2004JD004850, 2004.

1000 Mao, H. and Talbot, R.: Speciated mercury at marine, coastal, and inland sites in New England –  
1001 Part 1: Temporal variability, *Atmos. Chem. Phys.*, 12, 5099–5112, doi:10.5194/acp-12-5099-  
1002 2012, 2012.

1003 Mathur, R.: Estimating the impact of the 2004 Alaskan forest fires on episodic particular matter  
1004 pollution over the eastern United States through assimilation of satellite-derived aerosol optical

1005 depths in a regional air quality model, *J. Geophys. Res.-Atmos.*, 113, D17302,  
1006 doi:10.1029/2007JD009767, 2008.

1007 McKendry, I., Strawbridge, K., Karumudi, M. L., O'Neill, N., Macdonald, A. M., Leaitch,  
1008 R., Jaffe, D., Cottle, P., Sharma, S., Sheridan, P., and Ogren, J.: Californian forest fire plumes  
1009 over Southwestern British Columbia: lidar, sunphotometry, and mountaintop chemistry  
1010 observations, *Atmos. Chem. Phys.*, 11, 465–477, doi:10.5194/acp-11-465-2011, 2011.

1011 Miller, S. M., Matross, D. M., Andrews, A. E., Millet, D. B., Longo, M., Gottlieb, E. W., Hirsch,  
1012 A. I., Gerbig, C., Lin, J. C., Daube, B. C., Hudman, R. C., Dias, P. L. S., Chow, V. Y., and  
1013 Wofsy, S. C.: Sources of carbon monoxide and formaldehyde in North America determined from  
1014 high-resolution atmospheric data, *Atmos. Chem. Phys.*, 8, 7673–7696, doi:10.5194/acp-8-7673-  
1015 2008, 2008.

1016 Monks, P.: A review of the observations and origins of the spring ozone maximum, *Atmos.*  
1017 *Environ.*, 34, 3545–3561, doi:10.1016/S1352-2310(00)00129-1, 2000.

1018 Murazaki, K. and Hess, P.: How does climate change contribute to surface ozone change over  
1019 the United States?, *J. Geophys. Res.-Atmos.*, 111, 1–16, doi:10.1029/2005JD005873, 2006.

1020 Novelli, P. C., Masarie, K. A., Lang, P. M., Hall, B. D., Myers, R. C., and Elkins, J. W.:  
1021 Reanalysis of tropospheric CO trends: effects of the 1997–1998 wildfires, *J. Geophys. Res.-*  
1022 *Atmos.*, 108, ACH 14-1–ACH 14-14, 2003.

1023 Oltmans, S. J., Lefohn, A. S., Harris, J. M., and Shadwick, D. S.: Background ozone levels of air  
1024 entering the west coast of the US and assessment of longer-term changes, *Atmos. Environ.*, 42,  
1025 6020–6038, doi:10.1016/j.atmosenv.2008.03.034, 2008.

1026 Oltmans, S. J., Lefohn, A. S., Harris, J. M., Tarasick, D. W., Thompson, A. M., Wernli, H.,  
1027 Johnson, B. J., Novelli, P. C., Montzka, S. A., Ray, J. D., Patrick, L. C., Sweeney, C., Jefferson,



1028 A., Dann, T., Davies, J., Shapiro, M., and Holben, B. N.: Enhanced ozone over western North  
1029 America from biomass burning in Eurasia during April 2008 as seen in surface and profile  
1030 observations, *Atmos. Environ.*, 44, 4497–4509, doi:10.1016/j.atmosenv.2010.07.004, 2010.

1031 Oltmans, S. J., Lefohn, A. S., Shadwick, D., Harris, J. M., Scheel, H. E., Galbally, I., Tarasick, D.  
1032 W., Johnson, B. J., Brunke, E. G., Claude, H., Zeng, G., Nichol, S., Schmidlin, F., Davies, J.,  
1033 Cuevas, E., Redondas, A., Naoe, H., Nakano, T., and Kawasato, T.: Recent tropospheric ozone  
1034 changes – a pattern dominated by slow or no growth, *Atmos. Environ.*, 67, 331–351,  
1035 doi:10.1016/j.atmosenv.2012.10.057, 2013.

1036 Oswald, E. M., Dupigny-Giroux, L.-A., Leibensperger, E. M., Poirot, R., and Merrell, J.: Climate  
1037 controls on air quality in the northeastern U.S.: an examination of summertime ozone statistics  
1038 during 1993–2012, *Atmos. Environ.*, 112, 278–288, doi:10.1016/j.atmosenv.2015.04.019, 2015.

1039 Parrish, D. D., Singh, H. B., Molina, L., and Madronich, S.: Air quality progress in North  
1040 American megacities: a review, *Atmos. Environ.*, 45, 7015–7025,  
1041 doi:10.1016/j.atmosenv.2011.09.039, 2011.

1042 Parrish, D. D., Law, K. S., Staehelin, J., Derwent, R., Cooper, O. R., Tanimoto, H., Volz-Thomas,  
1043 A., Gilge, S., Scheel, H.-E., Steinbacher, M., and Chan, E.: Long-term changes in lower  
1044 tropospheric baseline ozone concentrations at northern mid-latitudes, *Atmos. Chem. Phys.*, 12,  
1045 11485–11504, doi:10.5194/acp-12-11485-2012, 2012.

1046 Parrish, D. D., Law, K. S., Staehelin, J., Derwent, R., Cooper, O. R., Tanimoto, H., Volz-  
1047 Thomas, A., Gilge, S., Scheel, H. E., Steinbacher, M., and Chan, E.: Lower tropospheric ozone at  
1048 northern midlatitudes: changing seasonal cycle, *Geophys. Res. Lett.*, 40, 1631–1636,  
1049 doi:10.1002/grl.50303, 2013.

1050 Pausata, F. S. R., Pozzoli, L., Vignati, E., and Dentener, F. J.: North Atlantic Oscillation and  
1051 tropospheric ozone variability in Europe: model analysis and measurements intercomparison,  
1052 *Atmos. Chem. Phys.*, 12, 6357–6376, doi:10.5194/acp-12-6357-2012, 2012.

1053 Penkett, S. A., Blake, N. J., Lightman, P., Marsh, A. R. W., Anwyl, P., and Butcher, G.: The  
1054 seasonal variation of nonmethane hydrocarbons in the free troposphere over the North  
1055 Atlantic Ocean: possible evidence for extensive reaction of hydrocarbons with the nitrate radical,  
1056 *J. Geophys. Res.*, 98, 2865–2885, 1993.

1057 Petrenko, V. V., Martinerie, P., Novelli, P., Etheridge, D. M., Levin, I., Wang, Z., Blunier, T.,  
1058 Chappellaz, J., Kaiser, J., Lang, P., Steele, L. P., Hammer, S., Mak, J., Langenfelds, R. L.,  
1059 Schwander, J., Severinghaus, J. P., Witrant, E., Petron, G., Battle, M. O., Forster, G., Sturges, W.  
1060 T., Lamarque, J.-F., Steffen, K., and White, J. W. C.: A 60 yr record of atmospheric carbon  
1061 monoxide reconstructed from Greenland firn air, *Atmos. Chem. Phys.*, 13, 7567–7585,  
1062 doi:10.5194/acp-13-7567-2013, 2013.

1063 Pfister, G., Hess, P. G., Emmons, L. K., Lamarque, J.-F., Wiedinmyer, C., Edwards, D. P.,  
1064 Pétron, G., Gille, J. C., and Sachse, G. W.: Quantifying CO emissions from the 2004 Alaskan  
1065 wildfires using MOPITT CO data, *Geophys. Res. Lett.*, 32, 1–5,  
1066 doi:10.1029/2005GL022995, 2005.

1067 Pollack, I. B., Ryerson, T. B., Trainer, M., Neuman, J. A., Roberts, J. M., and Parrish, D. D.:  
1068 Trends in ozone, its precursors, and related secondary oxidation products in Los Angeles,  
1069 California: a synthesis of measurements from 1960 to 2010, *J. Geophys. Res.-Atmos.*, 118,  
1070 5893–5911, doi:10.1002/jgrd.50472, 2013.

1071 Price, H. U., Jaffe, D. A., Cooper, O. R., and Doskey, P. V.: Photochemistry, ozone production,  
1072 and dilution during long-range transport episodes from Eurasia to the northwest United States, *J.*  
1073 *Geophys. Res.-Atmos.*, 109, 1–10, doi:10.1029/2003JD004400, 2004.

1074 Prinn, R. G.: The Cleansing Capacity of the Atmosphere, *Annu. Rev. Environ. Resour.*, 28, 29–  
1075 57, doi:10.1146/annurev.energy.28.011503.163425, 2003.

1076 Racherla, P. N. and Adams, P. J.: The response of surface ozone to climate change over the  
1077 Eastern United States, *Atmos. Chem. Phys.*, 8, 871–885, doi:10.5194/acp-8-871-2008, 2008.

1078 Real, E., Law, K. S., Weinzierl, B., Fiebig, M., Petzold, A., Wild, O., Methven, J., Arnold, S. A.,  
1079 Stohl, A., Huntrieser, H., Roiger, A. E., Schlager, H., Stewart, D., Avery, M. A., Sachse, G.  
1080 W., Browell, E. V., Ferrare, R. A., and Blake, D.: Processes influencing ozone levels in Alaskan  
1081 forest fire plumes during long-range transport over the North Atlantic, *J. Geophys. Res.-Atmos.*,  
1082 112, 1–19, doi:10.1029/2006JD007576, 2007.

1083 Reidmiller, D. R., Jaffe, D. A., Chand, D., Strode, S., Swartzendruber, P., Wolfe, G. M., and  
1084 Thornton, J. A.: Interannual variability of long-range transport as seen at the Mt. Bachelor  
1085 observatory, *Atmos. Chem. Phys.*, 9, 557–572, doi:10.5194/acp-9-557-2009, 2009.

1086 Rogers, J. C.: North Atlantic storm track variability and its association to the North Atlantic  
1087 oscillation and climate variability of northern Europe, *J. Climate*, 10, 1635–  
1088 1647, doi:10.1175/1520-0442(1997)010<1635:NASTVA>2.0.CO;2, 1997.

1089 Schwab, J. J., Spicer, J. B., and Demerjian, K. L.: Ozone, trace gas, and particulate matter  
1090 measurements at a rural site in southwestern New York state: 1995–2005, *J. Air Waste Manage.*,  
1091 59, 293–309, doi:10.3155/1047-3289.59.3.293, 2009.

1092 Serreze, M. C., Barrett, A. P., Slater, A. G., Steele, M., Zhang, J., and Trenberth, K. E.: The  
1093 large-scale energy budget of the Arctic, *J. Geophys. Res.-Atmos.*, 112, 1–17,  
1094 doi:10.1029/2006JD008230, 2007.

1095 Stevenson, D. S., Dentener, F. J., Schultz, M. G., Ellingsen, K., van Noije, T. P. C., Wild,  
1096 O., Zeng, G., Amann, M., Atherton, C. S., Bell, N., Bergmann, D. J., Bey, I., Butler, T., Cofala, J.,  
1097 Collins, W. J., Derwent, R. G., Doherty, R. M., Drevet, J., Eskes, H. J., Fiore, A. M., Gauss, M.,  
1098 Hauglustaine, D. A., Horowitz, L. W., Isaksen, I. S. A., Krol, M. C., Lamarque, J. F., Lawrence,  
1099 M. G., Montanaro, V., Müller, J. F., Pitari, G., Prather, M. J., Pyle, J. A., Rast, S., Rodriguez, J.  
1100 M., Sanderson, M. G., Savage, N. H., Shindell, D. T., Strahan, S. E., Sudo, K., and Szopa, S.:  
1101 Multimodel ensemble simulations of present-day and near-future tropospheric ozone, *J. Geophys.*  
1102 *Res.-Atmos.*, 111, D08301, doi:10.1029/2005JD006338, 2006.

1103 Stohl, A., Bonasoni, P., Cristofanelli, P., Collins, W., Feichter, J., Frank, A., Forster, C.,  
1104 Gerasopoulos, E., Gäggeler, H., James, P., Kentarchos, T., Kromp-Kolb, H., Krüger, B., Land,  
1105 C., Meloen, J., Papayannis, A., Priller, A., Seibert, P., Sprenger, M., Roelofs, G. J., Scheel, H.  
1106 E., Schnabel, C., Siegmund, P., Tobler, L., Trickl, T., Wernli, H., Wirth, V., Zanis, P., and  
1107 Zerefos, C.: Stratosphere–troposphere exchange: a review, and what we have learned from  
1108 STACCATO, *J. Geophys. Res.-Atmos.*, 108, 8516, doi:10.1029/2002JD002490, 2003.

1109 Talbot, R., Mao, H., and Sive, B.: Diurnal characteristics of surface level O<sub>3</sub> and other important  
1110 trace gases in New England, *J. Geophys. Res.-Atmos.*, 110, 1–16, doi:10.1029/2004JD005449,  
1111 2005.

1112 Thompson, D. W. J. and Wallace, J. M.: The Arctic oscillation signature in the wintertime  
1113 geopotential height and temperature fields, *Geophys. Res. Lett.*, 25, 1297,  
1114 doi:10.1029/98GL00950, 1998.

1115 Thompson, D. W. J. and Wallace, J. M.: Annular mode in the extratropical circulation. Part I:  
1116 Month-to-month variability, *J. Climate*, 13, 1000–1016, 2000.

1117 Tilmes, S., Lamarque, J.-F., Emmons, L. K., Conley, A., Schultz, M. G., Saunois, M., Thouret,  
1118 V., Thompson, A. M., Oltmans, S. J., Johnson, B., and Tarasick, D.: Technical Note:  
1119 Ozonesonde climatology between 1995 and 2011: description, evaluation and applications,  
1120 *Atmos. Chem. Phys.*, 12, 7475–7497, doi:10.5194/acp-12-7475-2012, 2012.

1121 Tohjima, Y., Kubo, M., Minejima, C., Mukai, H., Tanimoto, H., Ganshin, A., Maksyutov, S.,  
1122 Katsumata, K., Machida, T., and Kita, K.: Temporal changes in the emissions of CH<sub>4</sub> and CO  
1123 from China estimated from CH<sub>4</sub> / CO<sub>2</sub> and CO / CO<sub>2</sub> correlations observed at Hateruma Island,  
1124 *Atmos. Chem. Phys.*, 14, 1663–1677, doi:10.5194/acp-14-1663-2014, 2014.

1125 U.S. Environmental Protection Agency (EPA): Our Nation’s Air Status and Trends Through  
1126 2010, available at: <http://www3.epa.gov/airtrends/2011/>, 2012.

1127 U.S. Environmental Protection Agency (EPA): National Ambient Air Quality Standards for  
1128 Ozone; Proposed Rule, *Fed. Regist.*, 79, 75234, doi:10.2753/RSH1061-1983310140, 2014.

1129 West, J. J., Fiore, A. M., Horowitz, L. W., and Mauzerall, D. L.: Global health benefits of  
1130 mitigating ozone pollution with methane emission controls, *P. Natl. Acad. Sci. USA*, 103, 3988–  
1131 3993, doi:10.1073/pnas.0600201103, 2006.

1132 Wigder, N. L., Jaffe, D. A., and Saketa, F. A.: Ozone and particulate matter enhancements from  
1133 regional wildfires observed at Mount Bachelor during 2004–2011, *Atmos. Environ.*, 75, 24–31,  
1134 doi:10.1016/j.atmosenv.2013.04.026, 2013.

1135 Wild, O. and Akimoto, H.: Intercontinental transport of ozone and its precursors in a three-  
1136 dimensional global CTM, *J. Geophys. Res.-Atmos.*, 106, 27729–27744,  
1137 doi:10.1029/2000JD000123, 2001.

1138 Wilson, R. C., Fleming, Z. L., Monks, P. S., Clain, G., Henne, S., Konovalov, I. B., Szopa, S.,  
1139 and Menut, L.: Have primary emission reduction measures reduced ozone across Europe? An  
1140 analysis of European rural background ozone trends 1996–2005, *Atmos. Chem. Phys.*, 12, 437–  
1141 454, doi:10.5194/acp-12-437-2012, 2012.

1142 Woollings, T. and Blackburn, M.: The north Atlantic jet stream under climate change and its  
1143 relation to the NAO and EA patterns, *J. Climate*, 25, 886–902, doi:10.1175/JCLI-D-11-00087.1,  
1144 2012.

1145 Worden, H. M., Deeter, M. N., Frankenberg, C., George, M., Nichitiu, F., Worden, J., Aben, I.,  
1146 Bowman, K. W., Clerbaux, C., Coheur, P. F., de Laat, A. T. J., Detweiler, R., Drummond, J. R.,  
1147 Edwards, D. P., Gille, J. C., Hurtmans, D., Luo, M., Martínez-Alonso, S., Massie, S., Pfister, G.,  
1148 and Warner, J. X.: Decadal record of satellite carbon monoxide observations, *Atmos. Chem.*  
1149 *Phys.*, 13, 837–850, doi:10.5194/acp-13-837-2013, 2013.

1150 World Meteorological Organization: WMO Greenhouse Gas Bulletin: The State of Greenhouse  
1151 Gases in the Atmosphere Based on Global Observations through 2011, No 8, 4, 2012.

1152 Wotawa, G. and Trainer, M.: The influence of Canadian forest fires on pollutant concentrations  
1153 in the United States, *Science*, 288, 324–328, doi:10.1126/science.288.5464.324, 2000.

1154 Wotawa, G., Novelli, P. C., Trainer, M., and Granier, C.: Inter-annual variability of summertime  
1155 CO concentrations in the Northern Hemisphere explained by boreal forest fires in North America  
1156 and Russia, *Geophys. Res. Lett.*, 28, 4575–4578, doi:10.1029/2001GL013686, 2001.

1157 Xing, J., Pleim, J., Mathur, R., Pouliot, G., Hogrefe, C., Gan, C.-M., and Wei, C.: Historical  
1158 gaseous and primary aerosol emissions in the United States from 1990 to 2010, *Atmos. Chem.*  
1159 *Phys.*, 13, 7531–7549, doi:10.5194/acp-13-7531-2013, 2013.

1160 Xing, J., Mathur, R., Pleim, J., Hogrefe, C., Gan, C.-M., Wong, D. C., Wei, C., Gilliam, R., and  
1161 Pouliot, G.: Observations and modeling of air quality trends over 1990–2010 across the Northern  
1162 Hemisphere: China, the United States and Europe, *Atmos. Chem. Phys.*, 15, 2723–2747,  
1163 doi:10.5194/acp-15-2723-2015, 2015.

1164 Xu, X., Lin, W., Wang, T., Yan, P., Tang, J., Meng, Z., and Wang, Y.: Long-term trend of  
1165 surface ozone at a regional background station in eastern China 1991–2006: enhanced variability,  
1166 *Atmos. Chem. Phys.*, 8, 2595–2607, doi:10.5194/acp-8-2595-2008, 2008.

1167 Zhang, Q., Streets, D. G., Carmichael, G. R., He, K. B., Huo, H., Kannari, A., Klimont, Z., Park,  
1168 I. S., Reddy, S., Fu, J. S., Chen, D., Duan, L., Lei, Y., Wang, L. T., and Yao, Z. L.: Asian  
1169 emissions in 2006 for the NASA INTEX-B mission, *Atmos. Chem. Phys.*, 9, 5131–5153,  
1170 doi:10.5194/acp-9-5131-2009, 2009.

1171 Zhou, X., Huang, G., Civerolo, K., Roychowdhury, U., and Demerjian, K. L.: Summertime  
1172 observations of HONO, HCHO, and O<sub>3</sub> at the summit of Whiteface Mountain, New York, J.  
1173 *Geophys. Res.-Atmos.*, 112, 1–13, doi:10.1029/2006JD007256, 2007.

Table 1. Ground stations with geographical coordinates and measurement periods.

Site	Latitude	Longitude	Elevation	Measurement Period (CO)	Measurement Period (O <sub>3</sub> )
Appledore Island (AI)	42.97°N	70.62°W	18 m	Jul, 2001- Jul, 2011	Jul, 2002- Mar, 2012
Thompson Farm (TF)	43.11°N	70.95°W	23m	Apr, 2001- Jul, 2011	Apr, 2001- Aug, 2010
Mt. Washington (MWO)	44.27°N	71.30°W	1917m	Apr, 2001- Apr, 2009	Apr, 2001- May, 2010
Castle Spring (CS)	43.75°N	71.35°W	396m	Apr, 2001- Jun, 2008	Apr, 2001- May, 2008
Pack Monadnock (PM)	42.86°N	71.88°W	698m	Jun, 2004- Jul, 2011	Jul, 2004- Oct, 2008
Whiteface Mountain (WFM)	44.40°N	73.90°W	1484 m	Jan, 1996- Dec, 2010	Jan, 1996- Dec, 2010
Pinnacle State Park (PSP)	42.09°N	77.21°W	504 m	Jan, 1997- Dec, 2010	Jan, 1997- Dec, 2010

Note: CO and O<sub>3</sub> at AI were measured seasonally from May to September before 2007/2008. Year-round measurements of CO and O<sub>3</sub> began in May, 2007 and February, 2008, respectively.



Table 2. Trends (ppbv yr<sup>-1</sup>) of baseline CO and O<sub>3</sub> in spring, summer, fall, and winter. *p*-values are in the parentheses. Boldfaced numbers indicate *p*-value < 0.10.

Site	Period	Spring		Summer		Fall		Winter		Annual	
		CO	O <sub>3</sub>	CO	O <sub>3</sub>	CO	O <sub>3</sub>	CO	O <sub>3</sub>	CO	O <sub>3</sub>
AI	2002-2010			0.8(0.66)	<b>-3.1(0.07)</b>						
CS	2001-2008	3.4(0.06)	0.9(0.65)	2.4(0.19)	-2.9(0.14)	1.1(0.57)	1.5(0.45)	6.1(<0.01)	0.4(0.86)	<b>2.8(&lt;0.01)</b>	0.8(0.39)
MWO	2001-2009	-13.2(0.51)	-0.7(0.71)	<b>-4.5(0.01)</b>	<b>-4.7(0.01)</b>	<b>-4.4(0.01)</b>	-0.9(0.64)	-1.7(0.36)	0.1(0.98)	<b>2.3(&lt;0.01)</b>	0.7(0.42)
PM	2005-2010	<b>-6.5(&lt;0.01)</b>	-1.9(0.39)	<b>-5.5(&lt;0.01)</b>	-3.5(0.14)	<b>-4.2(0.05)</b>	-3.4(0.11)	<b>-5.5(0.01)</b>	0.1(1.00)	<b>3.5(&lt;0.01)</b>	0.8(0.43)
TF	2001-2010	<b>-3.7(0.02)</b>	<b>2.4(0.10)</b>	<b>-4.5(&lt;0.01)</b>	-0.1(0.94)	<b>-3.2(0.04)</b>	0.2(0.90)	<b>-4.8(&lt;0.01)</b>	<b>2.7(0.09)</b>	<b>2.5(&lt;0.01)</b>	0.8(0.29)
PSP	2001-2010	<b>-4.5(&lt;0.01)</b>	1.3(0.43)	<b>-4.3(&lt;0.01)</b>	-0.8(0.57)	<b>-4.2(0.01)</b>	-1.9(0.23)	<b>-3.9(0.02)</b>	-0.7(0.68)	<b>4.3(&lt;0.01)</b>	0.7(0.40)
WFM	2001-2010	-0.5(0.78)	0.4(0.83)	-1.9(0.23)	<b>-4.7(&lt;0.01)</b>	<b>-6.4(&lt;0.01)</b>	0.5(0.76)	-2.1(0.21)	-1.3(0.45)	<b>2.8(&lt;0.01)</b>	0.9(0.27)

Table 3. The contributions, in  $r^2R^2$ , of CO emissions from wildfires over Russia, Canada, Alaska, and California to variation ( $r^2$ ) in baseline CO at each site. The combined effect of wildfire emissions over Russia and Canada was also computed. Boldfaced numbers indicate  $p$ -value < 0.10.

	Russia		Canada		Alaska		California		Combined	
	$r^2R^2$	$p$	$r^2R^2$	$p$	$r^2R^2$	$p$	$r^2R^2$	$p$	$r^2R^2$	$p$
AI	<b>0.39</b>	<b>0.01</b>	0.12	0.15	0.13	0.19	0.12	0.21	<b>0.41</b>	<b>0.02</b>
CS	<del>-0.41</del>	<del>-0.01</del>	<del>-0.17</del>	<del>-0.09</del>	<del>-0.06</del>	<del>-0.38</del>	<del>&lt;0.01</del>	<del>-0.92</del>	<del>-0.41</del>	<del>-0.02</del>
MWO	<b>0.41</b>	<b>0.01</b>	0.13	0.15	0.01	0.77	<0.01	0.88	<b>0.43</b>	<b>0.02</b>
TF	<b>0.64</b>	<b>0.01</b>	<b>0.40</b>	<b>0.05</b>	0.01	0.80	0.03	0.52	<b>0.65</b>	<b>0.01</b>
PSP	0.11	0.18	0.15	0.11	0.09	0.27	<0.01	0.93	0.16	0.27
WFM	<b>0.32</b>	<b>0.01</b>	<b>0.32</b>	<b>0.01</b>	<0.01	0.90	0.01	0.69	<b>0.38</b>	<b>0.03</b>
Mean	<del>0.37</del>	<del>0.38</del>	0.22		<0.05		<0.03		0.41	

Note: PM was not included due to insufficient data; CS was not included, as mixing ratios of baseline CO at this site were unusually high over May 2003 – June 2008.

Table 4. Correlation coefficient (r) and p-value between the pairs of variables in March and April over 2001 – 2010.

<u>Pair of Variables</u>	<u>CS</u>	<u>MWO</u>	<u>PM</u>	<u>TF</u>	<u>PSP</u>	<u>WFM</u>
<u>NAO index vs Baseline O<sub>3</sub></u>	<u><b>-0.75 (0.03)</b></u>	<u><b>-0.68 (0.03)</b></u>	<u><b>-0.81 (0.03)</b></u>	<u><b>-0.81 (&lt;0.01)</b></u>	<u><b>-0.58 (0.06)</b></u>	<u><b>-0.51 (0.10)</b></u>
<u>NAO index vs Baseline CO</u>	=	<u>-0.51 (0.12)</u>	<u>-0.06 (0.46)</u>	<u>0.30 (0.22)</u>	<u>-0.14 (0.36)</u>	<u>-0.16 (0.34)</u>
<u>Relative humidity vs NAO index</u>	<u><b>0.85 (0.02)</b></u>	=	=	<u><b>0.64 (0.06)</b></u>	<u>0.23 (0.26)</u>	<u>0.40 (0.13)</u>
<u>Relative humidity vs Solar radiation flux</u>	=	=	=	<u><b>-0.67 (0.05)</b></u>	=	=
<u>Baseline O<sub>3</sub> vs Solar radiation flux</u>	=	=	=	<u><b>0.75 (0.03)</b></u>	=	=
<u>Surface wind speed vs NAO index</u>	<u><b>0.68 (0.06)</b></u>	<u><b>0.76 (0.02)</b></u>	=	<u><b>0.57 (0.09)</b></u>	<u>0.44 (0.12)</u>	=

Note: CO at CS was not included, .as mixing ratios of baseline CO at this site were unusually high over May 2003 – June 2008.

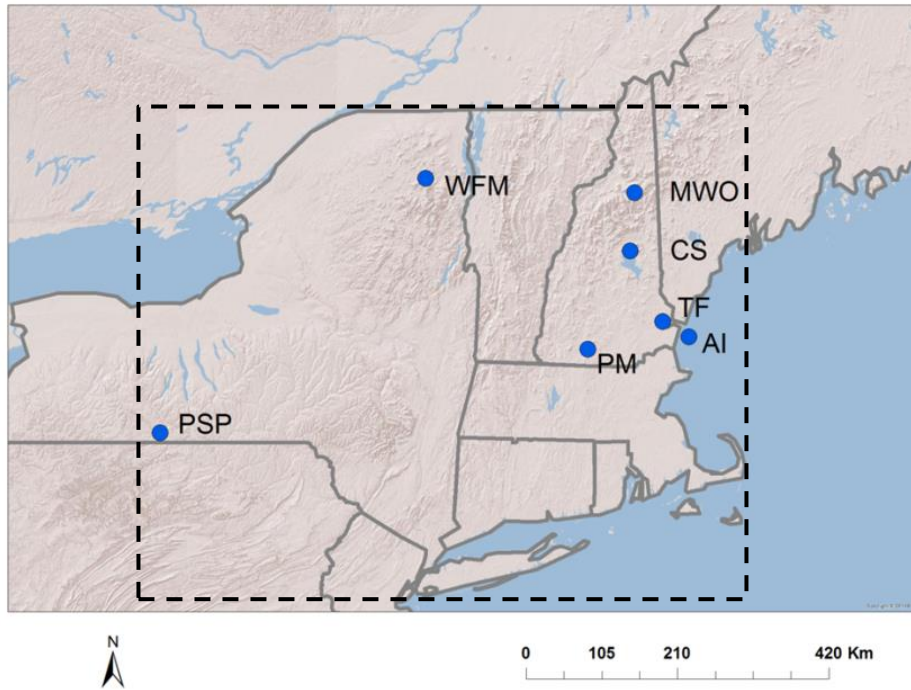


Fig. 1. Map of the Northeast U.S. The seven measurement sites used in the study are marked with blue dots.

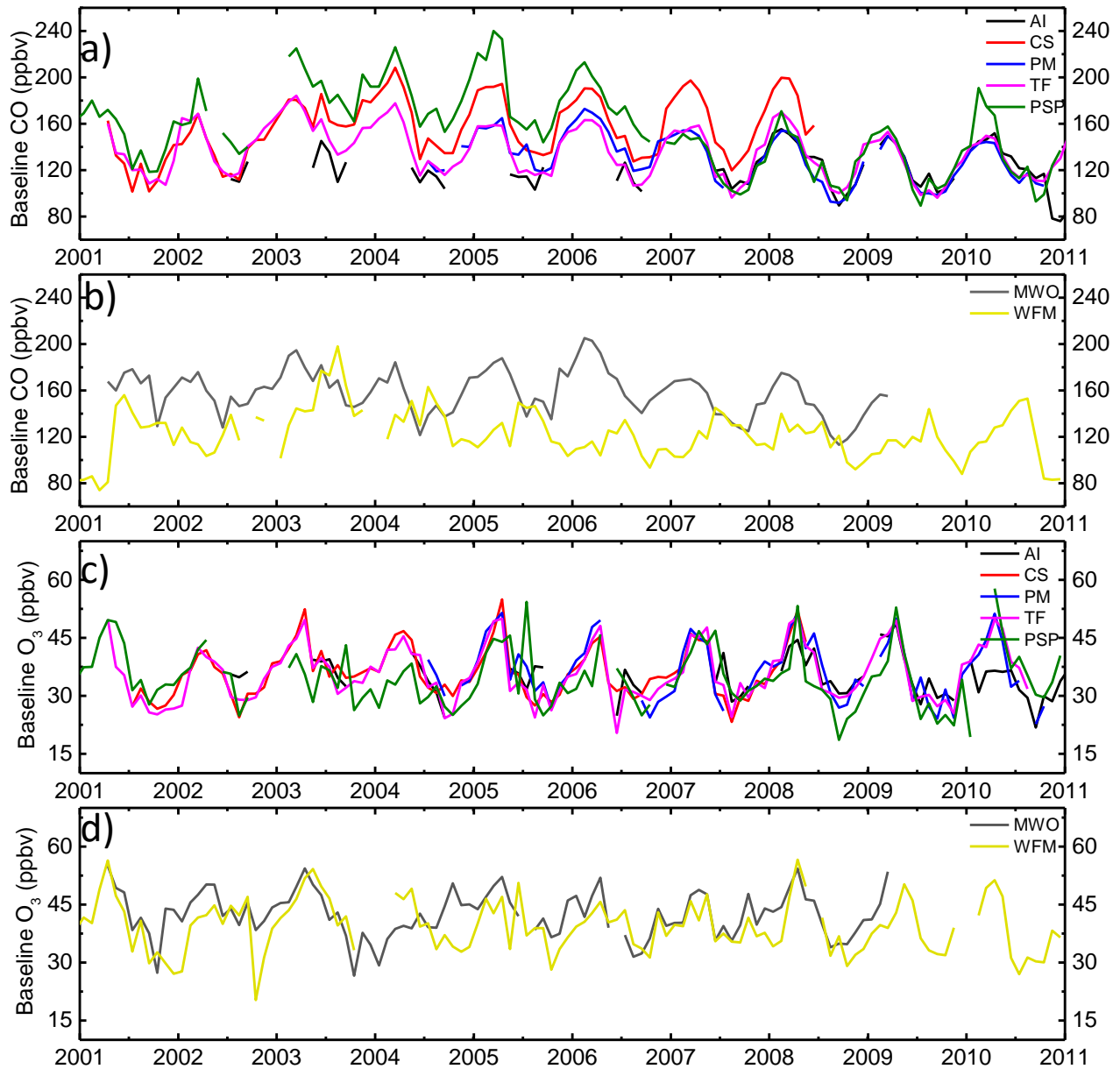


Fig. 2. Monthly baseline CO (ppbv) at (a) AI, CS, ~~MWO~~, PM, ~~and~~ TF, and PSP, and (b) MWO and WFMPSP. Monthly baseline O<sub>3</sub> (ppbv) at (c) AI, CS, ~~MWO~~, PM, ~~and~~ TF, and PSP, and (d) MWO and WFMPSP.

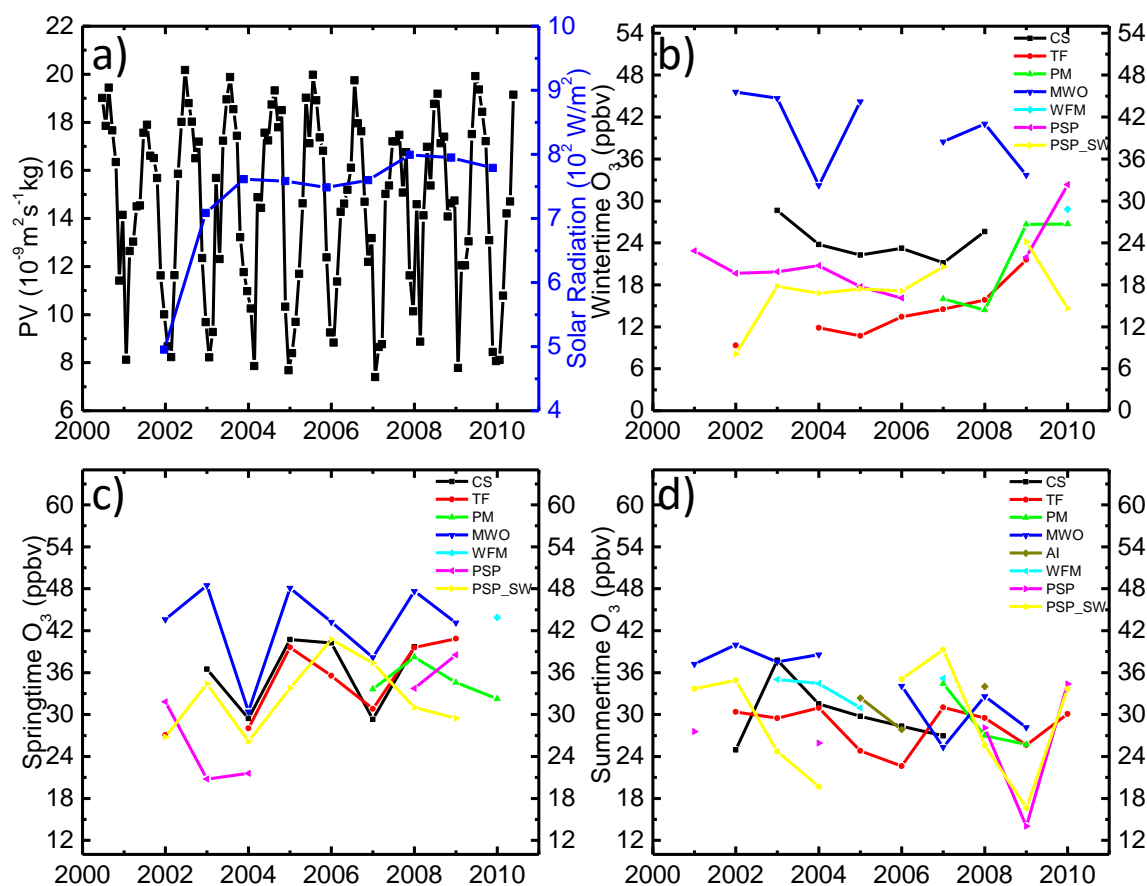


Fig. 3. (a) Time series of monthly PV ( $10^{-9} \text{ m}^2 \text{ s}^{-1} \text{ kg}$ ) at 350 K over the study region ( $40^{\circ}\text{N} - 45^{\circ}\text{N}$ ,  $70^{\circ}\text{W} - 77.5^{\circ}\text{W}$ ), indicated with dashed box in Fig. 1) and averaged daily maximum solar radiation flux at TF in spring (March, April, and May). Seasonal 10<sup>th</sup> percentile mixing ratios of O<sub>3</sub> with wind from the directions aligned with the urban corridor in (b) winter, (c) spring, and (d) summer. Specifically, the wind directions selected for AI:  $157.5^{\circ} - 202.5^{\circ}$ ; CS:  $157.5^{\circ} - 202.5^{\circ}$ ; MWO:  $157.5^{\circ} - 202.5^{\circ}$ ; PM:  $112.5^{\circ} - 157.5^{\circ}$ ; TF:  $157.5^{\circ} - 202.5^{\circ}$ ; WFM:  $112.5^{\circ} - 157.5^{\circ}$ ; PSP:  $67.5^{\circ} - 112.5^{\circ}$ . In addition, seasonal 10<sup>th</sup> percentile mixing ratios of O<sub>3</sub> at PSP with wind from the directions aligned with the Ohio River Valley was calculate as PSP\_SW ( $202.5^{\circ} - 247.5^{\circ}$ ) in (b), (c), and (d).

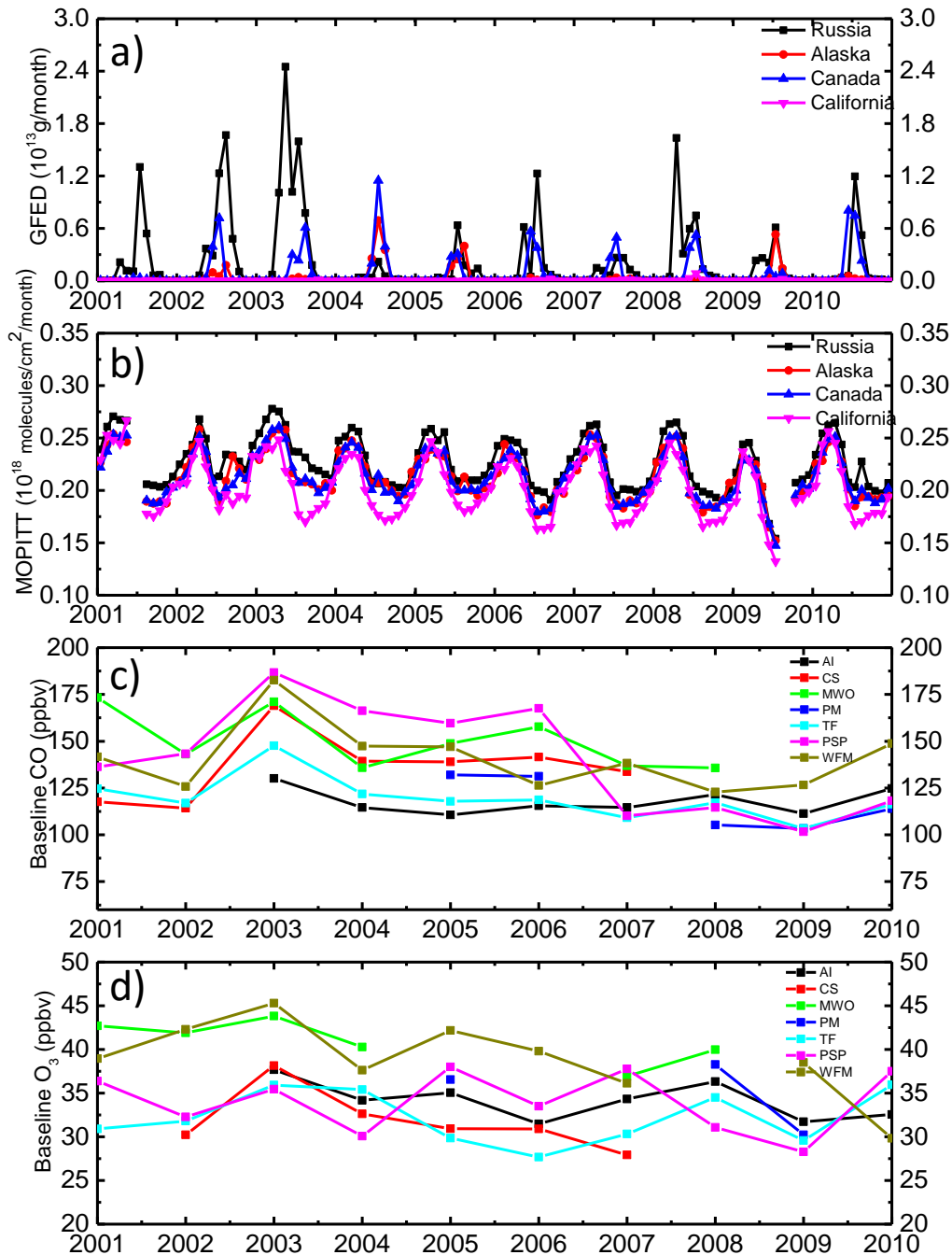


Fig. 4. (a) CO emissions from biomass burning based on GFED dataset. (b) Total CO columns based on MOPITT retrievals over Russia (black), Alaska (red), Canada (blue), and California (magenta). Summertime averaged baseline (c) CO and (d) O<sub>3</sub> at each site.

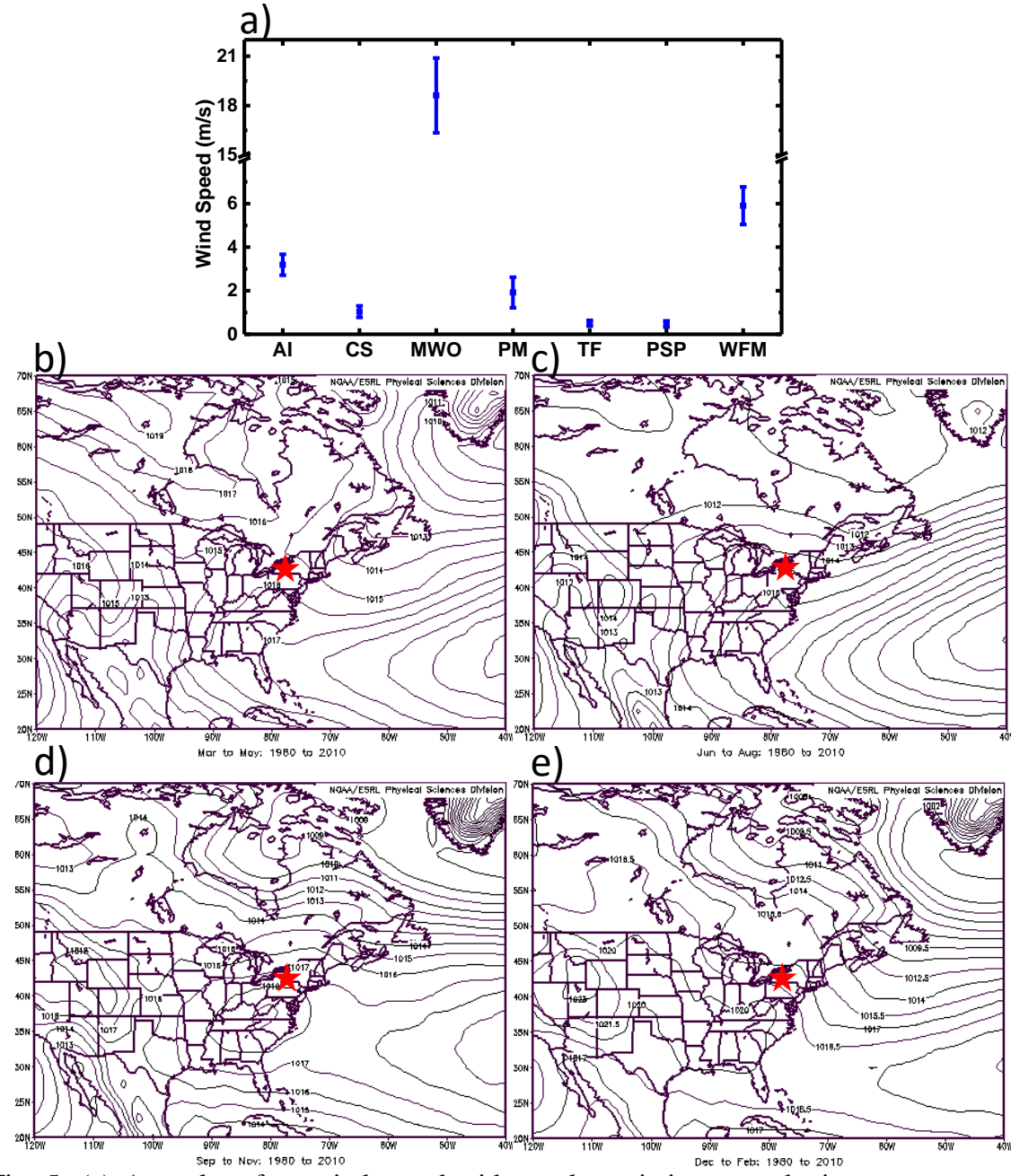


Fig. 5. (a) Annual surface wind speed with yearly variation at each site over summer 2001 – 2010. Northeast U.S. sea surface pressure (hPa) in (b) spring, (c) summer, (d) fall, and (e) winter. Red stars indicate the location of PSP.



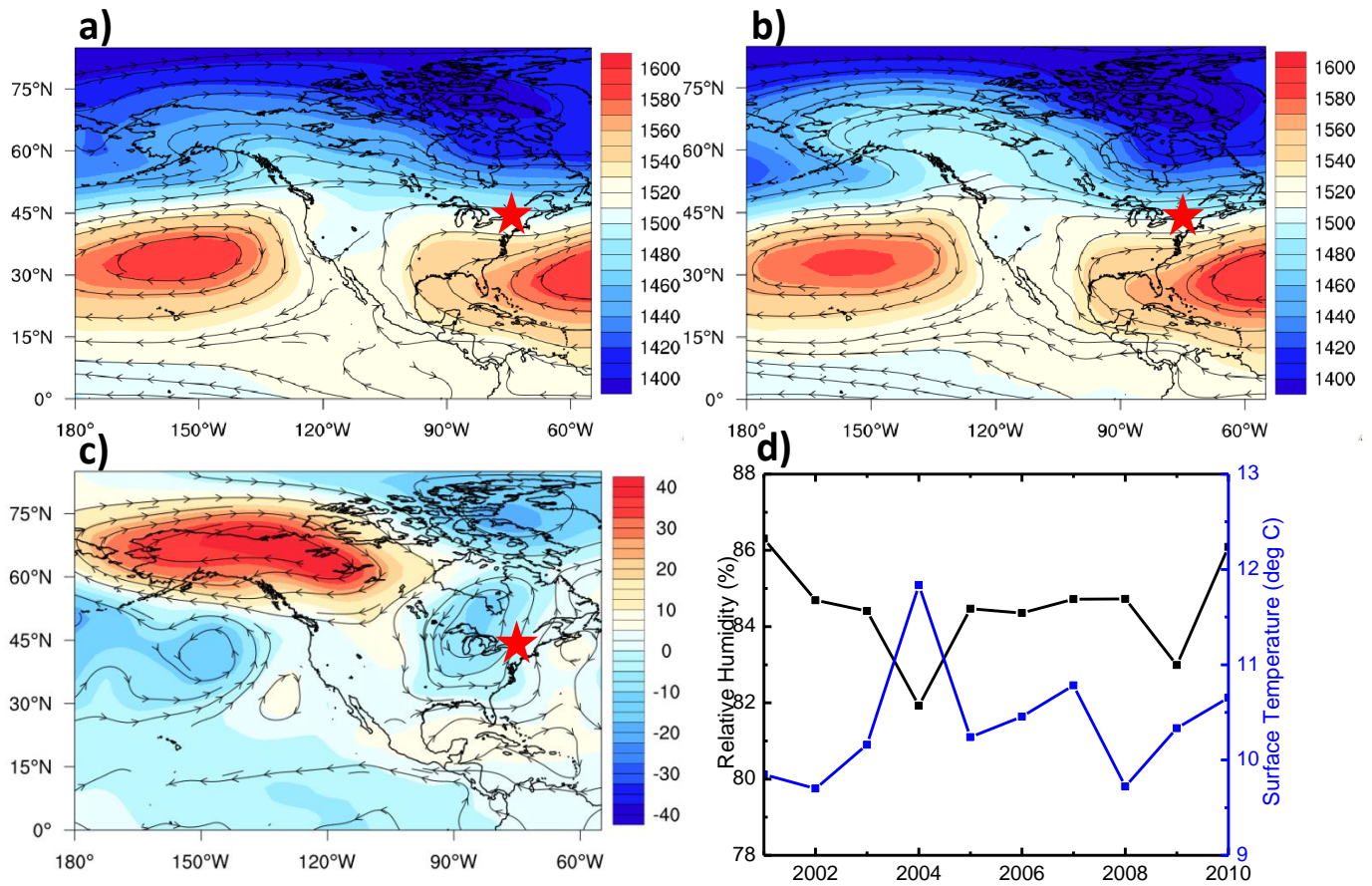


Fig. 6. Geopotential height at the 850 hPa pressure level during summer in (a) 2001-2010 (b) 2004. (c) The difference of geopotential height at 850 hPa between summer 2004 and the 10-year average. (d) The annual surface temperature and relative humidity over Alaska and southwestern Canada (55°N – 70°N, 110°W – 160°W) over summer 2001 – 2010. Red stars indicated the area of the study sites. (Source: NCEP/NCAR reanalysis)

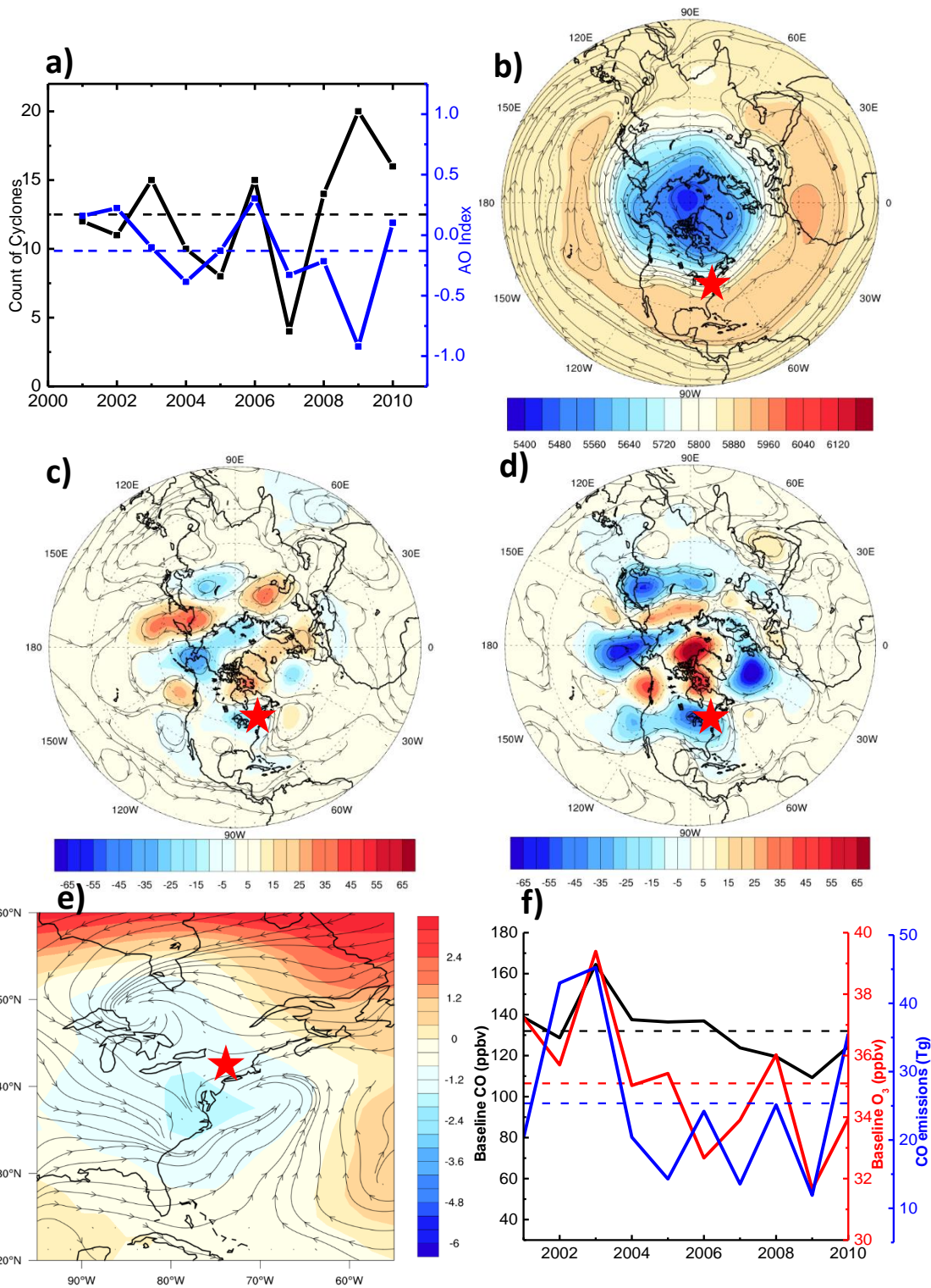


Fig. 7. (a) Counts of cyclones in the Northeast U.S. (black) and the AO index (blue) in summer. (b) Geopotential height at 500 hPa from the NCEP/NCAR reanalysis data during summer 2001 – 2010. (c) The difference of geopotential height at 500 hPa between years with strong (2003, 2006, 2008, 2009, and 2010) and weak (2001, 2002, 2004, 2005, and 2007) cyclone activities. (d) The difference of geopotential height at 500 hPa between summer 2009 and the 10-year means. (e) The difference of sea level pressure between summer 2009 and the 10-year means. (f) Time series of summertime baseline CO (black) and baseline O<sub>3</sub> (red) averaged over all seven sites, and Time series of CO emissions (blue) from wildfires in Russia and Canada. Dashlines indicate the 10-year means. Red stars indicate the area of the study sites.

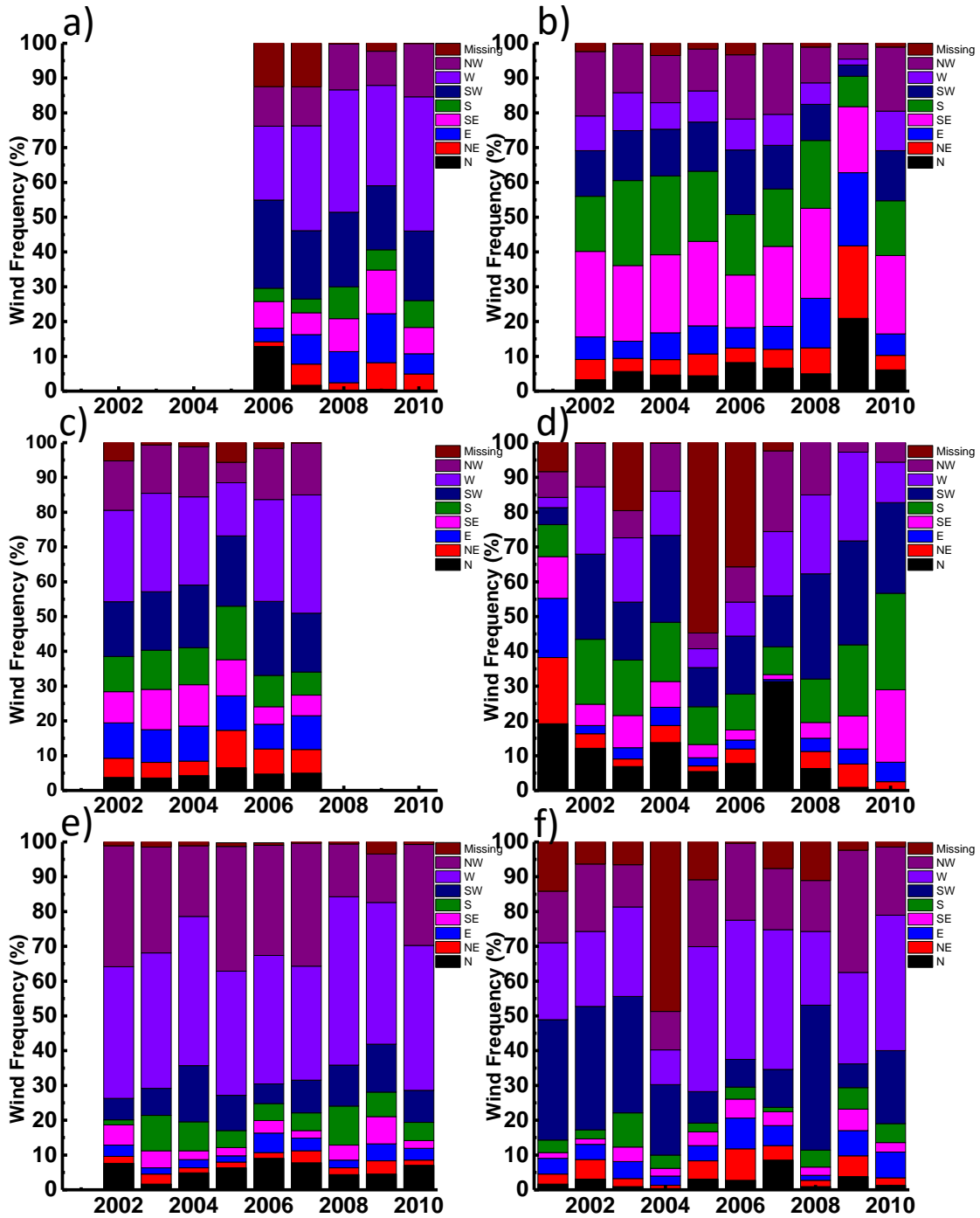


Fig. 8. Wind frequency in summer at (a) PM, (b) MWO, (c) CS, (d) WFM, (e) TF, (f) PSP. N:-  
 22.5° – 22.5°; NE: 22.5° – 67.5°; E: 67.5° – 112.5°; SE: 112.5° – 157.5°; S: 157.5° – 202.5°; SW:  
 202.5° – 247.5°; W: 247.5° – 337.5°; NW: 337.5° – -22.5°

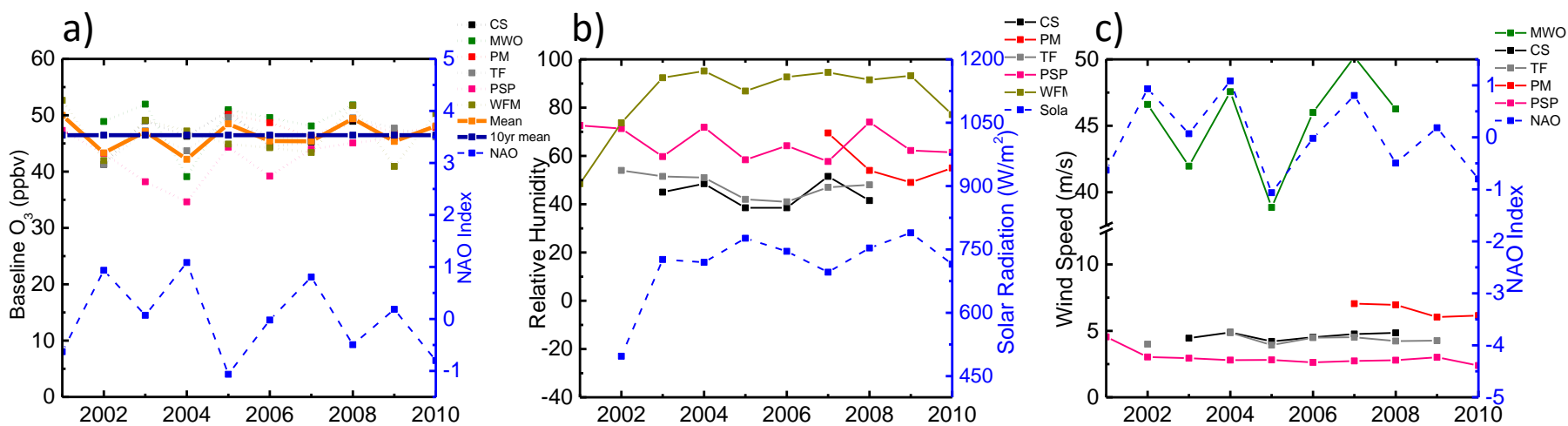


Fig. 9. (a) Baseline O<sub>3</sub> and the NAO index averaged in March and April. The thick orange line indicates the baseline O<sub>3</sub> averaged over the seven sites and the thick dark blue line indicates the mean value 46.5 ppbv over 2001 – 2010. (b) Averaged daytime (18:00 – 24:00 UT) relative humidity and daily maximum solar radiation flux at TF in March and April. (c) Averaged wind speed (> 2 m s<sup>-1</sup>) from the west (247.5° – 337.5°) and the NAO index in March and April.

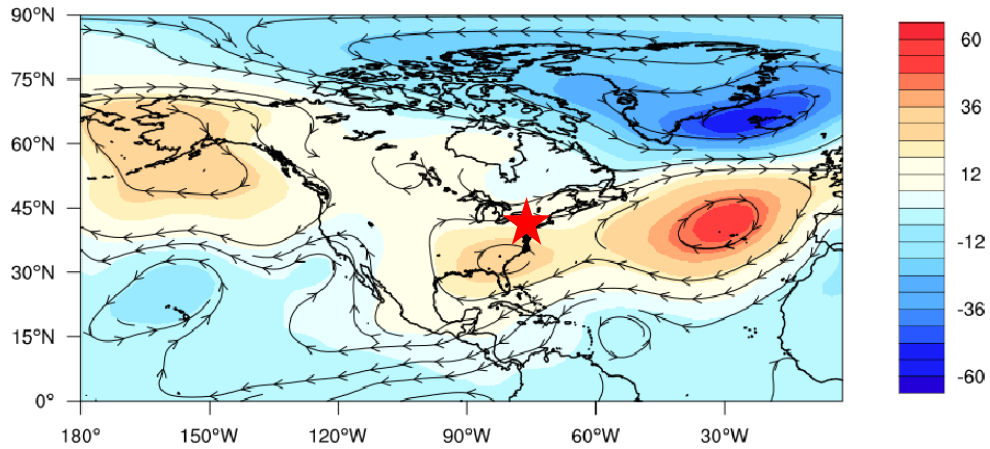


Fig. 10. The difference of geopotential height (m) and streamlines at 850-hPa between the low O<sub>3</sub> years (2002, 2004, 2006, 2007, and 2009) and high O<sub>3</sub> years (2001, 2003, 2005, 2008, and 2010). The red star indicates the area including the study sites.

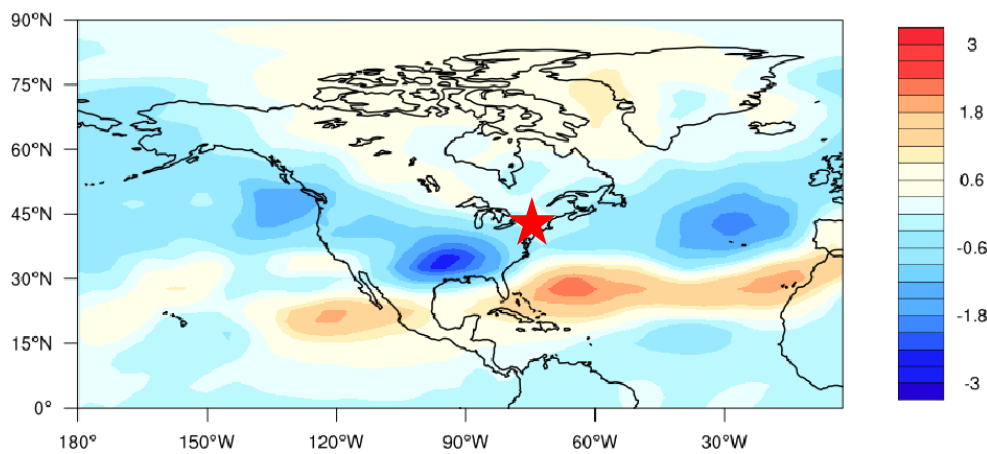


Fig. 11. Same as Fig. 10 except that the difference of PV ( $10^{-9} \text{ m}^2 \text{ s}^{-1} \text{ kg}$ ) at 350 K is shown.

